MICROCOPY RESOLUTION TEST CHART

NATIONAL BUREAU OF STANDARDS-1963-A

DTIC ①

AD-A151 900

ANALYSIS OF SPACE DIVERSITY TECHNIQUES

FOR EHF SATELLITE DOWNLINKS

THESIS

Steven L. Skipper
Captain, USAF

AFIT/GE/ENG/84D-61

DTIC
ELECTE
S
APR 0 2 1985
D
E

DEPARTMENT OF THE AIR FORCE
AIR UNIVERSITY
AIR FORCE INSTITUTE OF TECHNOLOGY

Wright-Patterson Air Force Base, Ohio

85    03    13    056

ANALYSIS OF SPACE DIVERSITY TECHNIQUES

FOR EHF SATELLITE DOWNLINKS

THESIS

Steven L. Skipper
Captain, USAF

AFIT/GE/ENG/84D-61

ANALYSIS OF SPACE DIVERSITY TECHNIQUES

FOR EHF SATELLITE DOWNLINKS

THESIS

Presented to the Faculty of the School of Engineering

of the Air Force Institute of Technology

Air University

In Partial Fulfillment of the

Requirements for the Degree of

Master of Science in Electrical Engineering

Steven L. Skipper, B.S.

Captain, USAF

December 1984

| Accession For | | |
|---|---|---|
| NTIS GRA&I | | X |
| DTIC TAB | | ☐ |
| Unannounced | | ☐ |
| Justification | | |
| By | | |
| Distribution/ | | |
| Availability Codes | | |
| | Avail and/or | |
| Dist | Special | |
| A-1 | | |

## Preface

The purpose of this study was to investigate different techniques for selecting the optimum downlink signal received by spatially diverse earth stations operating in the extremely high frequency (EHF) band. Space diversity configurations can be used to overcome the attenuation effects of rainfall, which can be very severe for frequencies above 10 GHz. Thus, special consideration must be given to the parameters and methods used to determine the optimum received signal when employing a space diversity reception system. This report is limited in scope to the development of three linear diversity combining techniques. The theoretical analysis and development of each of these techniques can be fully understood by the reader with a background in probability theory and digital signaling techniques.

I would like to thank Mr. Richard A. Williams of the Defense Communications Engineering Center (DCEC) for proposing this project. Gratitude is also due to Captain Jim Frazier, also from DCEC, for his assistance in arranging our visits to DCEC. Special thanks to my faculty advisor, Major Kenneth G. Castor of the Air Force Institute of Technology, for his guidance and understanding that greatly aided me in the completion of this study.

<div align="right">Steven L. Skipper</div>

# Table of Contents

## List of Figures

## List of Tables

## Abstract

This study investigated some of the diversity combining techniques that can be used with a space diversity downlink reception configuration to overcome the attenuation effects of rainfall. The diversity combining techniques selected for development and analysis were selection, equal gain, and maximal ratio combining. Each of these techniques were considered with two different digital signaling schemes, 8-ary phase-shift keying (PSK) and differentially encoded quadrature PSK (DQPSK), to form six distinct diversity technique/ signaling scheme combinations.

The analysis was accomplished by deriving the probability of bit error functions for 8-ary PSK and DQPSK and by developing the probability of density functions for each diversity technique under the assumption of a slowly fading Rayleigh channel. By taking the integral from zero to infinity of the product of the two functions for each diversity technique/ signaling scheme combination, the probability of bit error was calculated for each specified combination. The number of channels in the diversity system was varied to illustrate the trade-off between the improvement of bit error performance and cost. The results show the theoretical benefits attributed to the diversity combining techniques that can be employed in satellite communications systems. Additionally, information is provided to estimate the rain attenuation

given the rain rate so that its effects on bit error per-
formance can be obtained and compared to the case of no rain
attenuation.

## ANALYSIS OF SPACE DIVERSITY TECHNIQUES
## FOR EHF SATELLITE DOWNLINKS

## I. Introduction

### Background

The use of orbiting satellites has become an integral part of our world-wide communications and military command, control, and communications systems. A satellite communications system can be categorized as one of three basic types shown in Figure 1.1. System I shows an uplink from a ground-based earth station to the satellite, and a downlink from the satellite back to the destination earth station. The function of the satellite is to collect the electromagnetic fields from the signal transmitted by the sending earth station and retransmit the received signal to the other earth station.

System II shows a satellite crosslink between two satellites prior to the downlink transmission. System III shows a satellite relay system involving an earth station, a near-earth user (aircraft, ship, etc.) and a satellite. The system III configuration is of particular importance since it has many military applications. Regardless of which system configuration is employed, there are several atmospheric effects that can degrade the transmitted signal strength and reduce the capability of transmitting information via satellite.

1
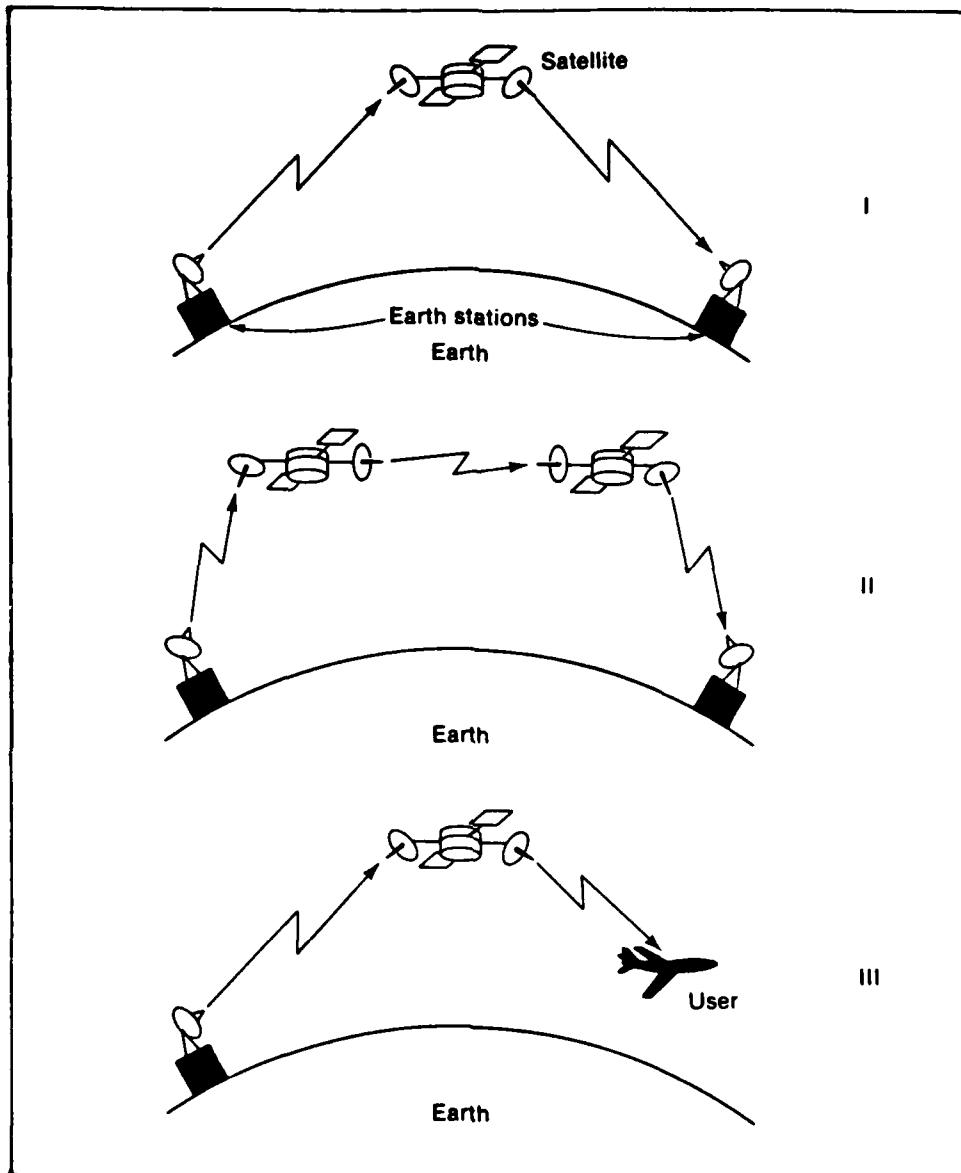
Figure 1.1    Types of Satellite Systems
          I    Ground-ground
         II    Ground-crosslink-ground
        III    Ground-user relay

                              Source: (11:5)

2

The most serious of these atmospheric effects to a satellite communications link is rainfall, which affects both uplink and downlink transmissions (11:96). Rain effects become more severe at wavelengths that approach the water drop size, which is dependent on the type of rainfall. In heavy rains as raindrop size increases, severe absorption occurs in the extremely high frequency (EHF) band, the range where many existing satellites operate. Therefore, in the EHF band, there is a potential for significantly more signal attenuation during rain as compared to the attenuation caused during clear weather conditions.

Generally, the solution to maintaining the satellite communications link is to add enough extra power (power margin) to transmit the signal over the maximum additional attenuation caused by rain. However, to maintain a highly reliable link in the EHF band, the cost of providing sufficient power margin with current technology becomes prohibitive and may not be technically feasible. One alternative for improving reliability is to spatially separate two or more earth stations since they are not likely to experience simultaneous fading from the same rainstorm (See Figure 1.2). For the uplink transmission, all earth station transmit the same signal and the optimum received signal (i.e., the signal with the least amount of attenuation) is chosen at the satellite and retransmitted. For the downlink reception, earth stations receive the transmitted signal from the satellite

3

Earth

(a)

Space Diversity in Uplink

Earth

(b)

Space Diversity in Downlink
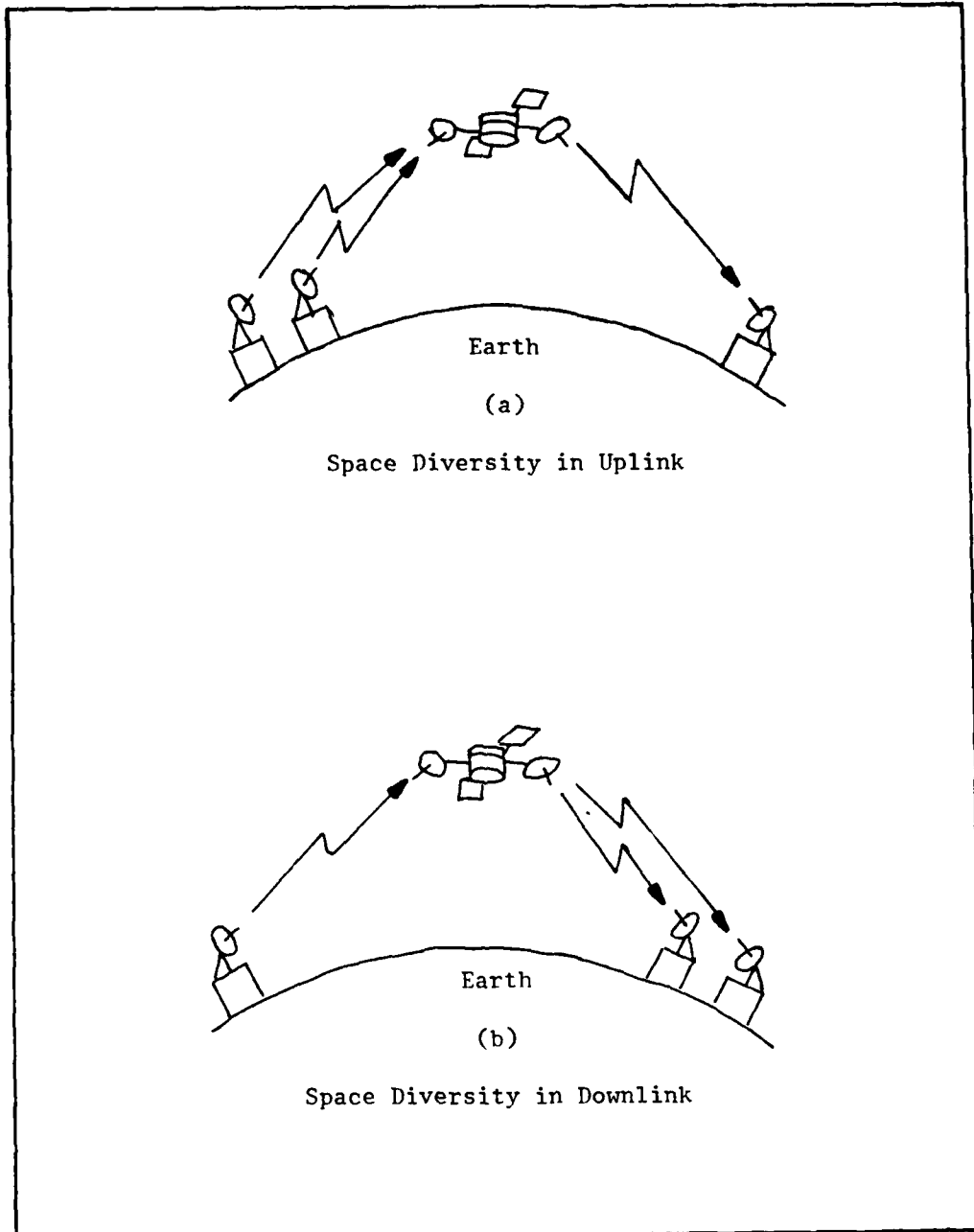
Figure 1.2    Using Space Diversity
in a Satellite System

simultaneously and the optimum signal is selected and then retransmitted to terrestrial destinations.

## Problem

When using a space diversity configuration to overcome the attenuation effects of rainfall, some consideration must be given to the parameters and the methods used to determine the optimum received signal. The purpose of this research is to investigate techniques for selecting the optimum signal from signals received by spatially diverse earth stations operating in the EHF band (i.e., the case of Figure 1.2b).

## Scope

The scope of this research will be limited to an investigation of methods to determine the optimum signal received by two or more spatially diverse earth stations from the satellite downlink transmissions. Different methods of selecting the optimum signal will be investigated and developed. After a theoretical analysis of each selection method, a computer program will be developed to simulate the operational environment and verify the best method for choosing the optimum received downlink signal in a space diversity configuration system. Costs associated with the development of the proposed methods for signal selection will not be examined.

## Assumptions

The following assumptions are made throughout this research project:

1. A satellite beacon is available.

2. All uplink transmissions are at 30 GHz and the down-link transmissions are at 20 GHz.

3. The focus of this report will be on satellite systems using diversity techniques to improve downlink reception performance as depicted in Figure 1.2b.

4. Digital signaling schemes used will be 8-ary Phase-Shift Keying (PSK) and Differentially encoded Quadrature PSK (DQPSK).

These assumptions are established to model a generic satellite system for military applications that could easily be developed and deployed using current satellite system technology and practices.

## Summary of Current Knowledge

The use of space diversity to combat atmospheric attenuation in satellite communications links is a well known concept that has been thoroughly researched and documented during the past 10-12 years (1,9). This research project will attempt to establish a model for space diversity gain by using well known linear diversity combining techniques and giving consideration to the spatial separation of the earth stations.

## Standards

The criterion used to measure the performance of each signal selection scheme will be the probability of bit error $(P_e)$ versus the average signal-to-noise ratio (SNR) per bit, $\gamma_b$, of the received downlink signal. This measurement is

the standard criterion for comparing the performances of digital communications systems. These values, $(P_e$ vs. $\gamma_b)$, will be calculated and plotted for each selection scheme during the computer simulation. These results will allow for a direct comparison of all of the developed signal selection schemes and a measurement of the benefits derived from using space diversity transmission schemes as compared to the result from the use of a standard satellite system without space diversity.

## Approach

A detailed investigation of possible linear diversity combining techniques for optimum signal selection will be conducted to determine which methods are best suited for this satellite communications application. For each diversity technique, the criteria for determining the optimum received signal will be fully developed. After a complete development and analysis of each of the proposed diversity signal selection methods, a computer simulation will model the operational environment and provide a performance measurement for each diversity technique.

## II. Satellite Background Information

The major elements in a satellite communications system include the satellite, a network of earth stations, and multiple-access communications equipment by which many earth stations can operate through a single satellite (22:131). A satellite communications link consists of a satellite orbiting in space and one or more earth stations. The performance of this communications link is greatly influenced by the earth-space propagation channel. One of the major differences between satellite links and terrestrial telecommunications is the distances that the carriers must be transmitted. Since the strength of the radiated signal diminishes with the square of the distance it travels, the satellite signals are relatively weak when received at the distant end. However, the amount of received carrier power determines the ability of the receiver to demodulate or decode the information (11:83). In satellite systems it is extremely important to know the key parameters that directly determine this received power so that these systems can be properly analyzed. Thus, an understanding of the basic power flow equations associated with satellite channels is necessary.

### Antenna Gain

The antennas used in satellite links do not radiate equally in all directions but are designed to focus the radiation in a particular direction. The increase in power

achieved by focusing the antenna is referred to as the gain of the antenna. An isotropic antenna which radiates equally in all directions has an antenna gain = 1. The gain of the antenna, $G_t(\phi_z, \phi_\ell)$ is a function of the angular direction of the receiver, where $(\phi_z, \phi_\ell)$ refers to the azimuth and elevation angle, respectively, measured from a coordinate system centered at the transmitting antenna (11:83). Therefore, antennas can be characterized by their gain pattern $G_t(\phi_z, \phi_\ell)$ which indicates how the antenna gain is distributed spatially with respect to the antenna coordinate system.

The most important parameters of an antenna pattern are its gain (the maximum value of the gain pattern), its beamwidth (a measure of the angle in which most of the gain occurs), and its sidelobes (amount of gain in the off-axis direction) (11:87). For most satellite communications purposes, antenna patterns should be highly directional with most of the gain concentrated over a narrow beamwidth and a very small part of the radiated energy in the sidelobes. However, the gain and beamwidth is dependent on the type of antenna used.

The gain of a transmitting antenna is

$$G_t = \frac{\text{Power received from the antenna}}{\text{Power received if the radiation were isotropic}} \quad (2.1)$$

Although the antenna gain is dependent on the type of antenna used, a useful approximation for this gain is

$$G = \frac{Z4\pi A_t}{\lambda^2} \quad (2.2)$$

9

where

> $A_t$ = aperture cross-sectional area of transmitting antenna

> $Z$ = the efficiency of the antenna aperture

> $\lambda$ = wavelength of transmission

$\lambda$, the wavelength of the radiation, is inversely proportional to its frequency f:

$$\lambda = \frac{C}{f} \qquad (2.3)$$

where C is the velocity of light. Thus, the antenna gain approximation can be written such that

$$G = \frac{Z4\pi f^2 A_t}{C^2} \qquad (2.4)$$

where

> $C = 2.99 \times 10^8$ meters/second

It *is obvious that the gain of the* antenna is dependent on the frequency of transmission and the efficiency of the antenna aperture.

## EIRP

The power of the transmitter is often referred to in a manner which takes the gain of the antenna into consideration. It is referred to as the effective isotropic radiated power (EIRP). EIRP is the power of a transmitter and isotropic antenna that would achieve the same result as the transmitter and antenna in question.

$$EIRP = P_t G_t (\phi_z, \phi_\ell) \qquad (2.5)$$

10

where

$P_t$ = available antenna input carrier power from the transmitter power amplifier, including circuit coupling losses and antenna radiation losses

$G_t(\phi_z, \phi_\ell)$ = gain of transmitting antenna

Now we can define the received carrier power collected by the receive antenna that is normal to the transmitter as

$$P_r = \frac{(EIRP)L_a A_r}{4\pi Z^2} \qquad (2.6)$$

where

$L_a$ = atmospheric loss

$A_r$ = the aperture of the receive antenna

$= (\lambda^2/4\pi)G_r(\phi_z', \phi_\ell') \qquad (2.7)$

where

$G_r(\phi_z', \phi_\ell')$ = azimuth and elevation angles of the transmitter relative to the receiver coordinate system

$\lambda$ = carrier wavelength

An equivalent expression for Eq (2.6) is

$$P_r = (EIRP)L_a L_p G_r(\phi_z', \phi_\ell') \qquad (2.8)$$

where we define

$$L_p = (\lambda/4\pi D)^2 = (C/4\pi fD)^2$$

$L_p$ is called the propagation or free space loss that is incurred by the communications link. It is dependent on the frequency, f, and the distance, D.

11

Eq (2.7) can also be restated in a more useful form where

$$(P_r)dB = (EIRP)dB + (L_p)dB + (L_a)dB + (G_r)dB \quad (2.9)$$

## External Noise

In addition to receiving the desired signal, the receiving antenna also gathers other forms of electromagnetic energy that may be present. These other radiations may be interference or noise that can distort the transmitted signal. The major external noises to a satellite communications link are:

1.  Atmospheric Losses/Noise

2.  Thermal Noise

3.  Sky Noise

4.  Galactic Noise

5.  Cosmic Noise

The combination of all sources of interference form a total noise level for the receiving system of the satellite link (16:123).

## Atmospheric Losses

There are many frequency dependent effects on the propagation channel, in addition to the free space loss, that increases the total transmission loss of the communications link (6:162). These propagation effects can be categorized as atmospheric losses. The primary causes of atmospheric losses for satellite communications links are:

12

1. uncondensed water vapor

2. molecular oxygen

3. rainfall

Water Vapor and Molecular Oxygen Attenuation. These
two losses are relatively constant and easily calculated,
although the attenuation levels vary within the carrier fre-
quency. The main reason for the attenuation due to water
vapor and molecular oxygen is that some of their associated
atmospheric particles have molecular resonances in the micro-
wave frequency band.

Below 10 GHz, atmospheric losses are minimal, (usually
less than 2 dB); however, at higher frequencies, the attenua-
tion begins to increase rapidly. The higher levels of atten-
uation occur at the frequencies having wavelengths corre-
sponding to specific gas molecules in the atmosphere (11:94).
Therefore, the attenuation caused by water vapor and oxygen
varies greatly with the frequency. Severe attenuation due to
water vapor molecules occurs at ~22 GHz while the severe
attenuation due to oxygen molecules occurs at ~60 GH. Thus,
the frequencies for the RF carrier for satellite links are
chosen in the frequency range where these types of attenua-
tion are minimized.

Rainfall Attenuation Effects. The effects of rainfall
attenuation on satellite communications varies with frequency,
however, it can have a severe effect on signal strength at
frequencies above 10 GHz. Rainfall is the most serious atmos-
pheric effect on a satellite link; therefore, special

consideration must be given to the effects of precipitation on the earth-space propagation path when designing a satellite communications system (8:2-1). At frequencies above 10 GHz, rain is known to cause significant attenuation, absorption, scattering, amplitude and phase scintillations, depolarization, and bandwidth decoherency. All of these phenomena combine to degrade the reliability of the satellite communications link. Its obvious impact on the satellite system is cost, since methods must be incorporated into the system to combat rainfall effects if uninterrupted service is desired (10:191).

Rainfall is a complicated subject primarily because of the complexity of the rainfall itself. Rainfall can assume many different forms depending on the geographical location, time of year, time of day, temperature, altitude, and other earth station site characteristics (8:2-1).

Types of Rain. As described in Ref 8, chapter 2, there are three basic types of rain: stratiform, convective, and cyclonic. In mid-latitude regions of the world, stratiform rain is a type of rain that primarily occurs in the spring and fall. It exhibits stratified horizontal extents of hundreds of kilometers (km), vertical heights of 4-6 km, with durations exceeding one hour and rain rates less than about 25 mm/hr (1 inch/hr). Stratiform rain has a rain rate and duration which often necessitates the use of link power margin to exceed the attenuation caused by a 25 mm/hr rain rate.

14

Convective rains are a result of vertical atmospheric motions producing vertical transport and mixing. The convective flow occurs in a cell whose horizontal extent is usually several kilometers. The cell usually extends to heights exceeding the freezing layer because of convective upwelling. The cell may be isolated or embedded in a thunderstorm associated with a weather front. Because of the motion of the front and the sliding motion of the cell along the front, the duration of high rain rate is usually only several minutes. This type of rain is the most common source of high rain rates in the U.S. and Canada.

Tropical cyclonic storms (hurricanes) occasionally pass along the U.S. eastern and southern coasts during August to October. These circular storms are typically 50-200 km in diameter, move at 10-20 km/hr, extend upward to 8 km, and have high rain rates that exceed 25 mm/hr.

Stratiform and cyclonic rainfall cover large geographic areas and the spatial distribution of total rainfall from such a storm is assumed to be uniform. Therefore, the rain rate averaged over several hours will be similar for earth stations located tens of kilometers apart (8:2-2). Convective storms are localized and generally produce non-uniform distributions of rainfall and rain rate for a given storm. The total rainfall and rain rate varies significantly over a distance of 10 km (8:2-2).

There are several proposed models for modeling the rainfall attenuation effects on satellite communications.

15

However, all of these models contain frequency dependent

coefficients and require the rain rate statistics for the

particular earth station sites since the rain rates vary with

location.  Currently, rain rate statistics are developed by

data collection experiments at the desired location.

Receiver Noise

In addition to the external noise collected by the

antenna, noise is also generated within the components of the

receiver immediately following the antenna.  The contribu-

tions from these sources of interference combine to define a

total noise level for the receiving system.  This noise level

set the minimal required power from the desire transmitter

to achieve reliable communications.

Noise Temperature.  The amount of receiver noise present

is defined by the receiver noise temperature, $T^{\circ}_{eq}$. This

parameter is an effective equivalent temperature that an

external noise source would need to produce to have the same

amount of receiver noise (11:101).

$$T^{\circ}_{eq} = T^{\circ}_{b} + (F-1)\ 290^{\circ} \qquad (2.10)$$

where

$T^{\circ}_{b}$ = background noise temperature accounting for con-
tributions collected by the antenna from external
sources

F = noise figure of receiver

A noise source of temperature $T^{\circ}_{eq}$ produces an effective

noise spectrum level at the antenna input of

16

$$N_o = KT^\circ_{eq} \quad \text{Watts/Hz} \qquad (2.11)$$

where

$$K = \text{Boltzmann's constant} = 1.379 \times 10^{-23} \text{ W/K-Hz}$$

$$= -228.6 \text{ dBW/K-Hz}$$

The total noise entering the receiver over a bandwidth, $B_{RF}$, is

$$P_n = KT^\circ_{eq}B_{RF} \qquad (2.12)$$

where

$B_{RF}$ = bandwidth of the receiver

Therefore, the total receiver noise can be calculated from the knowledge of the $T^\circ_{eq}$ of the receiver.

Noise Figure. The internal thermal noise is accounted for in $T^\circ_{eq}$ by specifying the receiver noise figure, F, which depends on the specific electronic circuit components following the antenna. The noise figure for an electronic system is defined as

$$F = \frac{\text{Total system output noise power}}{\text{Output system noise power due to system input noise at 290°K}} \qquad (2.13)$$

When defined as this, (F-1) 290°K is the temperature of an equivalent noise source at the system input that produces the same contribution to the system output noise as the internal noise of the system itself (11:103). For an example on the specifics on calculating F, see Ziemer and Tranter (23:478-81).

## Carrier-To-Noise Ratios (CNR)

One of the most useful indicators of the performance of a communications receiver is the ratio of the received carrier power to the total noise power of the receiver. This RF carrier-to-noise ratio (CNR) is defined as:

$$CNR = \frac{P_r}{P_n} \qquad (2.14)$$

where

$$P_r = (EIRP)L_p L_a G_r$$
$$P_n = KT^\circ_{eq} B_{eq}$$

The CNR indicates the relative strength of the desired transmitter-receiver power and the total noise interference (11:104). Eq (2.14) shows how the different link parameters affect receiver CNR. Since the receiver bandwidth $B_{RF}$ is often dependent on the modulation scheme, it is convenient to isolate the RF link power parameters by normalizing the CNR with respect to bandwidth. The resulting RF carrier-to-noise level ratio is defined as

$$(C/N_o) = (EIRP)L_p L_a G_r \qquad (2.15)$$

Obviously $(C/N_o)$ is now independent of $B_{RF}$. In a digital communications system, the $(C/N_o)$ ratio allows us to compute directly the receiver bit energy-to-noise level ratio as

$$E_b/N_o = (C/N_o)T_b \qquad (2.16)$$

where

$$T_b = \text{bit time}$$

18

By knowing the link $(C/N_o)$, which depends only on the RF link parameters, we can compute the analog CNR by dividing by $B_{RF}$ or the digital $E_b/N_o$ by multiplying by the bit time. It is convenient to express Eq (2.15) as

$$(C/N_o) = (EIRP/K) \ (L_p L_a) \ (G_r/T^\circ_{eq}) \qquad (2.17)$$

where

$\quad (EIRP/K) =$ transmitter parameter

$\quad (L_p L_a) =$ propagation parameter

$\quad (G_r/T^\circ_{eq}) =$ receiver parameter

Thus, each subsystem of the link contributes to the overall $(C/N_o)$. The only effect of the receiving system is the ratio $G_r/T^\circ_{eq}$. Therefore, as far as the receiver is concerned, performance can be maintained with a lower receiver gain (smaller antenna) if $T^\circ_{eq}$ (noise) can be reduced. There is a direct trade-off of receiver antenna size and receiver noise temperature in achieving a desired performance.

Power Link Equations

It is convenient to distinguish between the uplink and downlink transmission paths and their corresponding RF carrier-to-noise level ratios. The uplink equation can be described as

$$(C/N_o)_u = EIRP)_e - L_{pu} + G_r - T - K - L_{au} \quad dB\text{-}Hz \qquad (2.18)$$

where

$\text{EIRP)}_e$ = earth station EIRP, dBW

$L_{pu}$ = free space path loss, uplink, dB

$G_r$ = gain of the satellite receive antenna, dBi

$T$ = satellite receiver noise temperature, dB-K

$K$ = Boltzmann's constant = -228.6 dBW/K-Hz

$L_{au}$ = uplink atmospheric losses, dB

The downlink equation is described as

$$(C/N_o)_u = \text{EIRP)}_s - BO_o - L_{pd} + G_r - T - K - L_{ad} \quad (2.19)$$

dB-Hz

where

$\text{EIRP)}_s$ = satellite station EIRP, dBW

$BO_o$ = output backoff, dB

$L_{pd}$ = free space path loss, downlink, dB

$G_r$ = gain of the earth station receive antenna, dBi

$T$ = earth station receiver noise temperature, dB-K

$K$ = Boltzmann's constant = -228.6 dBW/K-Hz

$L_{ad}$ = downlink atmospheric losses, dB

Note: The output backoff term is expressed in dB from the saturated output point relative to saturated power. Since the power transfer function is nonlinear for the satellite transponder, $BO_o$ is a nonlinear function (2:14).

20

## Digital Signaling Methods for Satellite Communications Systems

In modern satellite communications systems, the trend has been towards digital instead of analog communications. A digital communication system transmits information waveforms that are first converted into a sequence of data symbols which are then transmitted over the satellite link by encoding onto RF carriers, (11:34), as depicted in Figure 2.1. A major advantage of digital communications is that information can be transmitted relatively error-free with less carrier power than is required for an analog system. For satellite systems, digital communications has the additional advantage that transmitted carrier waveforms can be carefully controlled in terms of amplitudes and frequency spectra, simplifying satellite hardware design (11:34).

The digital information to be transmitted over the channel is assumed to be a sequence of data symbols occurring at a uniform rate of R symbols/second. For binary signaling, the set of data symbols is restricted to a "1" bit and a "0" bit and each symbol may be transmitted directly by sending a waveform corresponding to a "1" or a waveform corresponding to a "0".

As an alternative to transmitting the binary bits directly, the information sequence can be grouped into blocks, where each block consists of k bits (19:140). With k bits/block, there are $2^k$ = M distinct blocks. Therefore, M different waveforms are needed to transmit the k-bit blocks unambiguously.
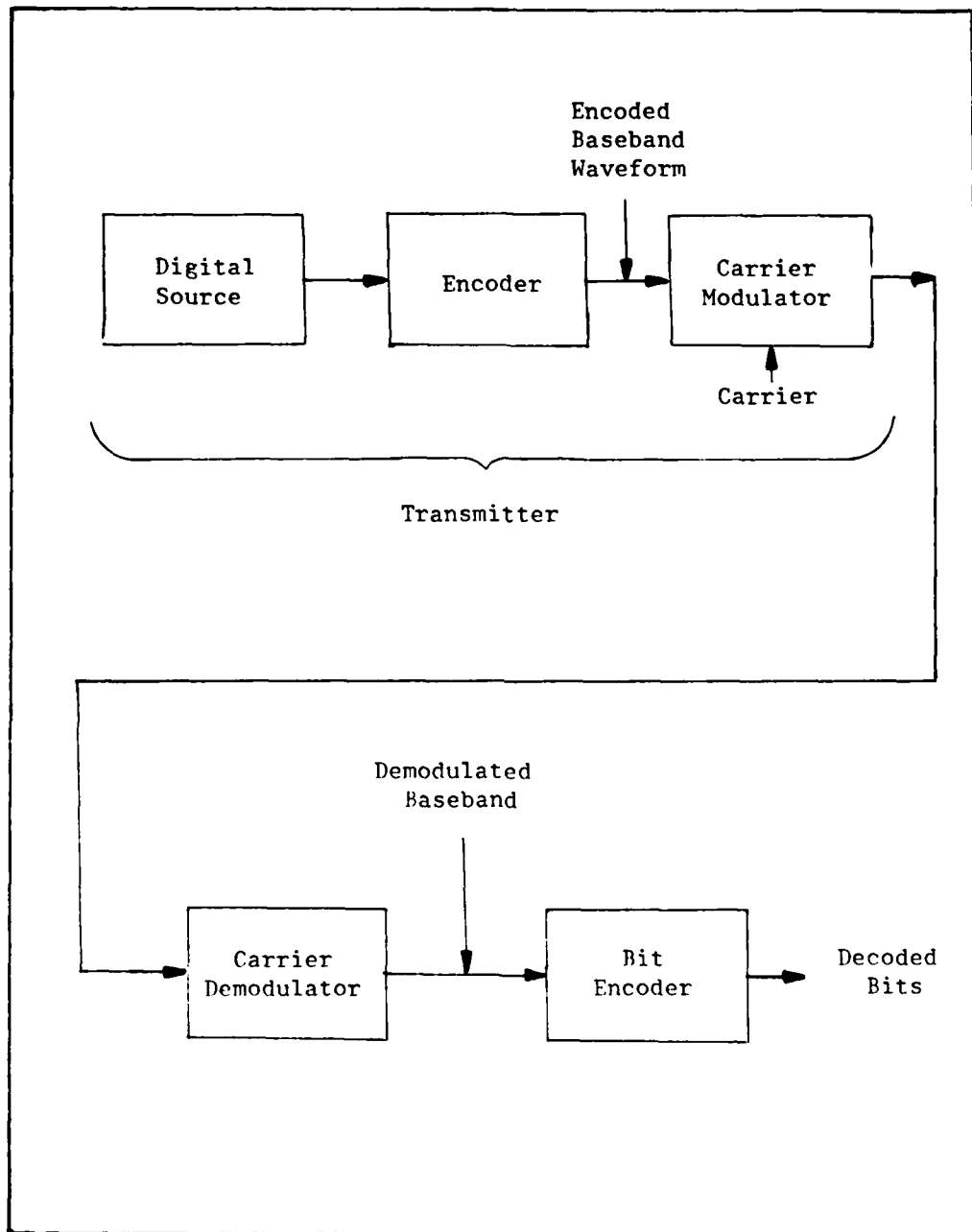
Figure 2.1   Digital Communications Block Diagram

Source: (11:35)

22

The commonly used measure of performance for digital communications systems is the relationship between bit error rate and signal-to-noise ratio (SNR) (2:38). The SNR for digital systems is usually expressed as the ratio energy per bit to the noise spectral density $(E_b/N_o)$. Generally, the desired modulation technique will be the one that satisfies the required system constraints and requires the least value for $E_b/N_o$ for a specified threshold error rate.

Digitals systems can be easily compared on the basis of ideal bit error rate. In comparing digital satellite communications systems the ideal bit error rate is used to determine the best possible performance. The following assumptions are made for the "ideal bit error rate" conditions (2:39):

1.  No phase or frequency uncertainties are introduced by earth station or satellite oscillators.

2.  No forward error correcting codes are used.

3.  Carrier and clock recovery is perfect, so that there is no recovered carrier phase or clock jitter.

4.  The only source of errors is the addition of random additive white gaussian noise by the channel.

Multiphase Signaling Waveforms. In a general M-ary signaling system, the possible transmitted signal waveforms may be denoted as $\{s_m(t)\}, m = 1, 2, \ldots, M$. We shall consider these waveforms to be bandpass signals, and represent them as

$$s_m(t) = Re[U_m(t) \exp(j\pi f_c t)] \qquad (2.20)$$

where

$$m = 1,2,\ldots M$$

$$\{u_m(t)\} = \text{the equivalent low-pass waveforms}$$

$$\text{Re} = \text{the real part of}$$

The M signals are characterized individually by their energy, defined as,

$$\mathcal{E}_m = \int_0^T s_m^2(t) \, dt$$

$$= 0.5 \int_0^T |u_m(t)|^2 \, dt \qquad (2.21)$$

where

$$m = 1,2,\ldots M$$

Note: We shall assume that all M signaling waveforms have equal energy such that

$$\mathcal{E} = \mathcal{E}_m \qquad (2.22)$$

where

$$m = 1,2,\ldots M$$

For M-ary phase shift keying (PSK), the baseband signaling waveforms $\{s_m(t)\}$ are used to phase modulate the RF carrier. The general representation for a set of M-ary phase signaling waveforms is

$$s_m(t) = \text{Re}\{u(t) \exp j(2\pi f_c t + (2\pi(m-1)/M) + \lambda)\} \qquad (2.23)$$

where

$$m = 1,2, \ldots, M$$

$$0 < t < T$$

$$\lambda \text{ is a fixed initial phase}$$

24

If u(t) = A,   0 < t < T

and

u(t) = 0,    otherwise

then $s_m(t)$ may be expressed as a PSK signal

$$s_m(t) = A\cos[2\pi f_c t + (2\pi(m-1)/M) + \lambda] \qquad (2.24)$$

where

m = 1,2,...M

0 < t < T

<u>Performance of M-ary PSK</u>.  The probability of bit/symbol
error analysis is thoroughly presented in Proakis, (Ref 19,
Chap 4).  The results of this analysis are:

Case 1:  M = 2,   PSK Waveforms = Antipodal Waveforms

$$P_b = Q[(2\gamma_b)^{0.5}] \qquad (2.25)$$

where

$P_b$ = probability of bit error

$\gamma_b = E_b/N_o$ = SNR per bit

$$Q(x) = 1 - \int_{-\infty}^{x}(1/(2\pi)^{0.5}) \exp(-B^2/2) \, dB \qquad (2.25.a)$$

Case 2:  M = 4,   $\lambda = \pi/4$

$$P_m = 2Q[(2\gamma_b)^{0.5}] - [Q(2\gamma_b)^{0.5}]^2 \qquad (2.26)$$

where

$P_m$ = probability of k-bit symbol error

25

Case 3:  For $M \geq 8$ and $\gamma_b \geq 10$ dB

$$P_m = 2Q((2K\gamma_b)^{0.5} \sin (\pi/M)) \qquad (2.27)$$

$$P_b = P_m/k \qquad (2.28)$$

Differentially Encoded PSK (DPSK).  Ordinary PSK re-
quires coherent processing and accuracy constraints on
estimating the phase increase as M increases.  A procedure
which allows for easier phase and symbol synchronization is
called differential PSK.  In M-ary DPSK, instead of trans-
mitting signals with phases corresponding to the M possible
k-tuples, we transmit phases corresponding to the change
(difference) between the previous k-tuple and the current
k-tuple (4:V-65).

Performance of DPSK.

For $M = 2$:

$$P_b = 0.5 \exp(-\gamma_b) \qquad (2.29)$$

For $M = 4$:

$$P_b = Q(a,b) - 0.5I_o(ab)\exp\left[0.5(a^2 + b^2)\right] \qquad (2.30)$$

where

$$Q(a,b) = \exp[0.5(a^2 + b^2)] \sum_{K=0}^{\infty} (a/b)^K I_K(ab), \text{ for } b > a > 0$$

$$I\alpha(x) = \sum_{K=0}^{\infty} \frac{(x/2)^{\alpha + 2K}}{K! \ \Gamma(\alpha + K + 1)} , \ X \geq 0$$

$$a = 1.0824 \ (0.5\gamma_b)^{0.5}$$

$$b = 2.6131 \ (0.5\gamma_b)^{0.5}$$

## III. Rainfall Characteristics

Rainfall has a significant effect on satellite communications at frequencies above 10 GHz. Due to the scattering effect by rain which causes attenuation, depolarization, and interference, the characteristics of rain became an important parameter to satellite communications systems designers. In order to understand and appreciate the problem of rainfall attenuation, it is vital to discuss the basic characteristics of rain and its associated statistics.

### Rainfall Physical Structure Characteristics

The variability of rain with respect to space and time has been documented as early as the 1950's (1:369). Measurements on the ground have shown that differences in rainfall intensities can occur within distances of a few hundred feet. The understanding of the formation and distribution of large raindrops and high rainfall rates is of great importance to the designers of communications satellite systems.

Heavy rain usually occurs with cellular structures of limited horizontal and vertical extent (1:369). An important characteristic of raincells is their tendency to form into groups of cells within a region called a small mesoscale area which can be 100-400 $km^2$. As many as seven cells have been observed in a small mesoscale area and up to six small mesoscales areas within a large mesoscale area which is about 1000 $km^2$. The variations of the cell distribution with a

28

mesoscale structure are not purely random; the form of the mesoscale pattern can be greatly influenced by local climatological, meteorological, or topographical effects (1:369). The lifetime of rain showers and thunderstorms is longer than those of an individual cell; however, the lifetime of a single cell can vary greatly from as little as a few minutes to as long as several hours. The dynamics of raincells appear to fall into two basic categories: those in which the rainfall intensity within the cell is well preserved over periods of minutes while the cell itself moves across the terrain, and those in which the cells are basically stationary but exhibit large fluctuations in rainfall intensity with time (1:369).

## Rain Rates

Rain is normally measured as the rate (mm/hr) at which the rainfall is collected by a horizontal surface near the ground at the location of interest. Therefore, in order to obtain the rain rate of a particular location, an experiment designed to obtain these statistics must be performed at that location. Since rain varies greatly with time, the raw data contains too much information to be useful, thus the data is processed to reveal the long-term statistical characteristics of rain. The most important of these is the cumulative distribution function (CDF) (10:199), which shows the fraction of time a certain rain rate is not exceeded (see Figure 3.1).
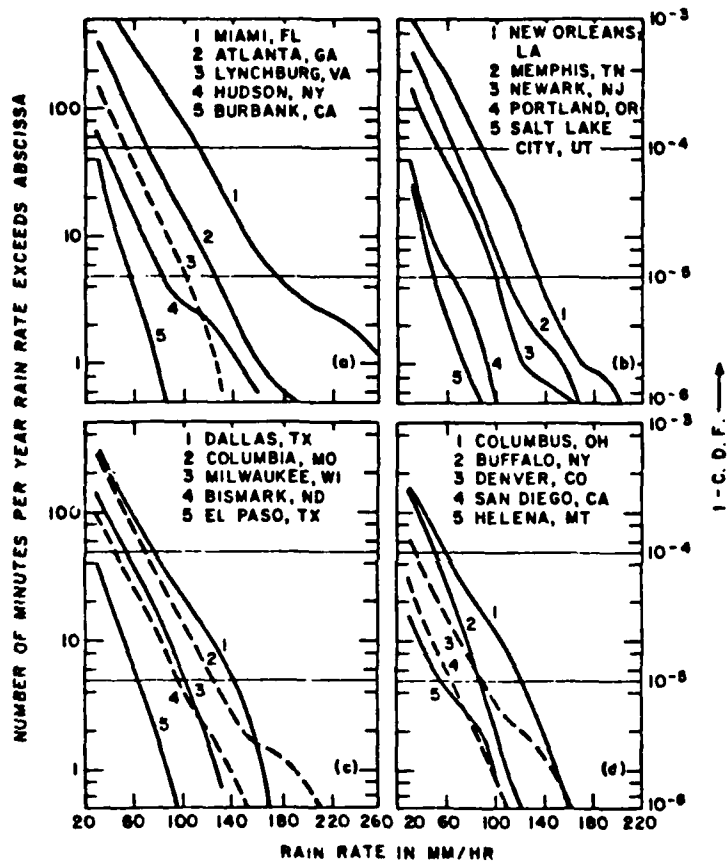
Figure 3.1    Cumulative Distribution Function (C.D.F.) of
              Rain Rates for 20 U.S. Locations During the
              Period 1966 to 1970; Based on One-Minute Intervals


                                              Source: (10:200)


30

In addition, for each rain rate, a typical distribution of drop sizes in a volume of space above and near the rain gauge can be determined as a function of the observed instantaneous rain rate (10:193). Although several rainfall distributions have been developed, some of the more common average dropsize distributions used in rain attenuation calculations are (19:321):

1. Laws and Parsons Distribution: This tabular distribution has been found to be a reasonable measure for an average dropsize spectrum in continental temperate rainfall. It is probably the most widely used distribution currently available.

2. Marshall-Palmer Distribution: This negative exponential distribution is a fairly good fit for the average dropsize spectrum. It is most applicable to the widespread rain in continental temperate climates although it has a tendency to overestimate the number of small drops.

3. "Thunderstorm" Distribution of Joss et. al.: This negative exponential distribution was fitted to the average dropsize spectrum measured in convective rain.

4. "Drizzle" Distribution of Joss et. al.: This negative exponential distribution was obtained by fitting the average dropsize spectrum of very light widespread rain composed mostly of small drops.

A typical Laws and Parson dropsize distribution of raindrop diameters and velocities for various rain rates is shown in Table 3.1.

31

TABLE 3.1

Measured Raindrop Terminal Velocities and Dropsize Distributions at Ground Level

Rain Rate (mm/hour)

Percent of Total Volume

| Drop Diameter (cm) | 0.25 | 1.25 | 2.5 | 5 | 12.5 | 25 | 50 | 100 | 150 | Terminal Velocity ($\frac{m}{sec}$) |
|---|---|---|---|---|---|---|---|---|---|---|
| 0.05 | 28.0 | 10.9 | 7.3 | 4.7 | 2.6 | 1.7 | 1.2 | 1.0 | 1.0 | 2.1 |
| 0.1 | 50.1 | 37.1 | 27.8 | 20.3 | 11.5 | 7.6 | 5.4 | 4.6 | 4.1 | 3.9 |
| 0.15 | 18.2 | 31.3 | 32.8 | 31.0 | 24.5 | 18.4 | 12.5 | 8.8 | 7.6 | 5.3 |
| 0.2 | 3.0 | 13.5 | 19.0 | 22.2 | 25.4 | 23.9 | 19.9 | 13.9 | 11.7 | 6.4 |
| 0.25 | 0.7 | 4.9 | 7.9 | 11.8 | 17.3 | 19.9 | 20.9 | 17.1 | 13.9 | 7.3 |
| 0.3 | | 1.5 | 3.3 | 5.7 | 10.1 | 12.8 | 15.6 | 18.4 | 17.7 | 7.9 |
| 0.35 | | 0.6 | 1.1 | 2.5 | 4.3 | 8.2 | 10.9 | 15.0 | 16.1 | 8.35 |
| 0.4 | | 0.2 | 0.6 | 1.0 | 2.3 | 3.5 | 6.7 | 9.0 | 11.9 | 8.70 |
| 0.45 | | | 0.2 | 0.5 | 1.2 | 2.1 | 3.3 | 5.8 | 7.7 | 9.0 |
| 0.5 | | | | 0.3 | 0.6 | 1.1 | 1.8 | 3.0 | 3.6 | 9.2 |
| 0.55 | | | | | 0.2 | 0.5 | 1.1 | 1.7 | 2.2 | 9.35 |
| 0.6 | | | | | | 0.3 | 0.5 | 1.0 | 1.2 | 9.5 |
| 0.65 | | | | | | | 0.2 | 0.7 | 1.0 | 9.6 |
| 0.7 | | | | | | | | | 0.3 | |

(10:193)

32

## Rain Scattering

In order to calculate a specific attenuation factor that corresponds to a specific rain rate, one must understand the phenomena of rain scattering. When rain particles enter the path of the satellite communications downlink signal, the particles both absorb and scatter the radiation associated with the transmitted signal. The interaction between the rain particles and the electromagnetic field associated with the signal can be satisfactorily computed by using electromagnetic scattering theory. However, exact solutions for the scattering problem are only available for simple shapes and distributions of the dielectric properties of the scatterer within the scatterer (7:176). Rain attenuation may be reasonably modeled using spheres with the assumptions that water is a homogeneous lossy dielectric, the drops are randomly distributed with a volume in accordance with a Poisson process, and the drop size distribution is known (6:460). More complex models of raindrops have been developed to account for the nonspherical physical description of rain but these models have only been partially successful and only at lower rain rates (7:176).

## Rain Attenuation Models

The most fundamental quantity in the calculation of rain attenuation statistics for space-earth paths is the attenuation per unit distance, A. There are two general approaches commonly used to calculate A, a theoretical technique and an

empirical method based upon the approximate relationship between A and the rain rate R. Both methods rely on the solution of the scattering problem by Mie (17:377, 7:176, 18:318-9). The validity of the theoretical approach is well established (18:318) and its calculations have been conducted for a wide variety of frequencies. However, the complexity of this approach makes it unsuitable for use by satellite communications systems designers.

The theoretical analysis of the rain attenuation results in the expression

$$A = 4.343 \int_{0}^{\infty} Q_t(D) \ N(D) dD \qquad (3.1)$$

where

$$Q_t = (4\pi/k^2) \ Re[S(0,D)]$$

$$S(0,D) = forward \ scattering \ amplitude$$

$$N(D) dD = number \ density \ of \ raindrops \ with \ equivalent$$
$$diameter \ D \ in \ the \ interval \ dD$$

Although it was believed that this equation included only the effects of single scattering, it also included the effects of all the forward multiple scattering processes (i.e., those processes which all paths between scatterers have components in the forward direction) (18:319). As suggested by Hogg and Chu (14:1310-2), these are the only multiple scattering processes which significantly contribute to the coherent rain attenuation.

The second method of calculating the rain attenuation is based on the approximation

34

$$A = aR^b \qquad (3.2)$$

where

        a,b = functions of frequency, raindrop size distribution, and rain temperature

This expression serves as a good approximation for the full Mie solution obtained in the theoretical approach for frequencies greater than 1 GHz and is suitable for most design applications. The difficulty with this method is obtaining accurate values for the coefficients a and b. Many methods for obtaining the coefficients have been developed including linear (b=1) and nonlinear relations, values for the coefficients at different frequencies by fitting the results of Mie calculations, and experimentally obtained empirical values for a and b (18:318). As expected, there are minor discrepancies in the values for these coefficients. An often used set of coefficient values is presented by Olsen, Rogers, and Hodges (18). This method presents a complete set of values of a and b for frequencies 1-1000 GHz where the values of specific attenuation obtained at several rain rates were used to determine a and b by means of logrithmic regression for different combinations of frequency, dropsize distribution, and temperature (See Tables 3.2, 3.3, 3.4).

## Statistical Behavior of Rain

In addition to the models to calculate a rain attenuation factor, there has been attempts to characterize the behavior of rain attenuation. One such effort is the work by

## TABLE 3.2

### Regression Calculations For a and b in
### $A = aR^b$ (dB/km) as Functions of Frequency
### and Dropsize Distribution with Rain Temperature = 20°C

| FREQ. (GHz) | a | | | | | b | | | | |
|---|---|---|---|---|---|---|---|---|---|---|
| | $LP_L$ | $LP_H$ | MP | J-T | J-D | $LP_L$ | $LP_H$ | MP | J-T | J-D |
| 1.0 | $3.84 \times 10^{-5}$ | $3.17 \times 10^{-5}$ | $5.14 \times 10^{-5}$ | $2.82 \times 10^{-5}$ | $5.17 \times 10^{-5}$ | 0.889 | 0.945 | 0.852 | 0.896 | 0.843 |
| 1.5 | $8.52 \times 10^{-5}$ | $6.75 \times 10^{-5}$ | $1.14 \times 10^{-4}$ | $5.53 \times 10^{-5}$ | $1.14 \times 10^{-4}$ | 0.905 | 0.972 | 0.867 | 0.960 | 0.846 |
| 2.0 | $1.53 \times 10^{-4}$ | $1.15 \times 10^{-4}$ | $2.02 \times 10^{-4}$ | $7.8 \times 10^{-5}$ | $2.03 \times 10^{-4}$ | 0.926 | 1.007 | 0.887 | 1.065 | 0.850 |
| 2.5 | $2.42 \times 10^{-4}$ | $1.73 \times 10^{-4}$ | $3.19 \times 10^{-4}$ | $8.29 \times 10^{-5}$ | $3.20 \times 10^{-4}$ | 0.951 | 1.049 | 0.913 | 1.234 | 0.856 |
| 3.0 | $3.57 \times 10^{-4}$ | $2.39 \times 10^{-4}$ | $4.64 \times 10^{-4}$ | $1.01 \times 10^{-4}$ | $4.67 \times 10^{-4}$ | 0.980 | 1.096 | 0.943 | 1.357 | 0.863 |
| 3.5 | $4.99 \times 10^{-4}$ | $3.11 \times 10^{-4}$ | $6.40 \times 10^{-4}$ | $1.01 \times 10^{-4}$ | $6.46 \times 10^{-4}$ | 1.013 | 1.151 | 0.981 | 1.533 | 0.870 |
| 4.0 | $6.73 \times 10^{-4}$ | $3.78 \times 10^{-4}$ | $8.4 \times 10^{-4}$ | $2.45 \times 10^{-4}$ | $8.59 \times 10^{-4}$ | 1.052 | 1.219 | 1.025 | 1.451 | 0.878 |
| 5.0 | $1.12 \times 10^{-3}$ | $5.15 \times 10^{-4}$ | $1.38 \times 10^{-3}$ | $7.49 \times 10^{-4}$ | $1.40 \times 10^{-3}$ | 1.150 | 1.377 | 1.122 | 1.414 | 0.898 |
| 6.0 | $1.79 \times 10^{-3}$ | $1.06 \times 10^{-3}$ | $2.13 \times 10^{-3}$ | $2.17 \times 10^{-3}$ | $2.13 \times 10^{-3}$ | 1.238 | 1.393 | 1.209 | 1.305 | 0.921 |
| 7.0 | $2.82 \times 10^{-3}$ | $2.04 \times 10^{-3}$ | $3.26 \times 10^{-3}$ | $4.59 \times 10^{-3}$ | $3.06 \times 10^{-3}$ | 1.284 | 1.380 | 1.255 | 1.236 | 0.945 |
| 8.0 | $4.34 \times 10^{-3}$ | $3.78 \times 10^{-3}$ | $4.8 \times 10^{-3}$ | $1.01 \times 10^{-2}$ | $4.25 \times 10^{-3}$ | 1.299 | 1.342 | 1.280 | 1.114 | 0.972 |
| 9.0 | $6.44 \times 10^{-3}$ | $6.74 \times 10^{-3}$ | $7.10 \times 10^{-3}$ | $1.55 \times 10^{-2}$ | $5.73 \times 10^{-3}$ | 1.296 | 1.285 | 1.274 | 1.076 | 0.998 |
| 10 | $9.20 \times 10^{-3}$ | $1.11 \times 10^{-2}$ | $1.01 \times 10^{-2}$ | $1.90 \times 10^{-2}$ | $7.52 \times 10^{-3}$ | 1.280 | 1.229 | 1.260 | 1.079 | 1.024 |
| 11 | $1.27 \times 10^{-2}$ | $1.67 \times 10^{-2}$ | $1.37 \times 10^{-2}$ | $2.42 \times 10^{-2}$ | $9.67 \times 10^{-3}$ | 1.259 | 1.181 | 1.244 | 1.060 | 1.047 |
| 12 | $1.68 \times 10^{-2}$ | $2.33 \times 10^{-2}$ | $1.81 \times 10^{-2}$ | $3.25 \times 10^{-2}$ | $1.22 \times 10^{-2}$ | 1.236 | 1.142 | 1.223 | 1.022 | 1.067 |
| 15 | $3.28 \times 10^{-2}$ | $4.59 \times 10^{-2}$ | $3.57 \times 10^{-2}$ | $5.89 \times 10^{-2}$ | $2.20 \times 10^{-2}$ | 1.173 | 1.076 | 1.160 | 0.966 | 1.106 |
| 20 | $6.83 \times 10^{-2}$ | $8.59 \times 10^{-2}$ | $7.51 \times 10^{-2}$ | 0.103 | $4.56 \times 10^{-2}$ | 1.111 | 1.044 | 1.103 | 0.934 | 1.123 |
| 25 | 0.113 | 0.143 | 0.127 | 0.181 | $7.76 \times 10^{-2}$ | 1.075 | 1.007 | 1.064 | 0.868 | 1.119 |
| 30 | 0.168 | 0.228 | 0.191 | 0.273 | 0.118 | 1.044 | 0.955 | 1.032 | 0.816 | 1.113 |
| 35 | 0.235 | 0.337 | 0.269 | 0.360 | 0.167 | 1.009 | 0.904 | 0.999 | 0.782 | 1.107 |
| 40 | 0.312 | 0.452 | 0.360 | 0.439 | 0.225 | 0.972 | 0.864 | 0.966 | 0.757 | 1.101 |
| 50 | 0.484 | 0.648 | 0.572 | 0.610 | 0.368 | 0.901 | 0.815 | 0.900 | 0.708 | 1.082 |
| 60 | 0.652 | 0.775 | 0.796 | 0.771 | 0.541 | 0.845 | 0.794 | 0.847 | 0.667 | 1.055 |
| 70 | 0.802 | 0.850 | 1.01 | 0.814 | 0.735 | 0.803 | 0.785 | 0.807 | 0.663 | 1.020 |
| 80 | 0.934 | 0.902 | 1.21 | 0.810 | 0.936 | 0.771 | 0.780 | 0.772 | 0.671 | 0.985 |
| 90 | 1.03 | 0.938 | 1.39 | 0.876 | 1.14 | 0.751 | 0.776 | 0.744 | 0.656 | 0.952 |
| 100 | 1.09 | 0.958 | 1.53 | 0.995 | 1.33 | 0.738 | 0.774 | 0.721 | 0.627 | 0.920 |
| 110 | 1.13 | 0.972 | 1.64 | 1.09 | 1.50 | 0.729 | 0.772 | 0.705 | 0.606 | 0.891 |
| 120 | 1.17 | 0.982 | 1.74 | 1.11 | 1.66 | 0.721 | 0.771 | 0.693 | 0.599 | 0.865 |
| 150 | 1.33 | 1.02 | 1.96 | 1.02 | 2.05 | 0.692 | 0.768 | 0.667 | 0.615 | 0.807 |
| 200 | 1.50 | 1.06 | 2.09 | 0.993 | 2.47 | 0.664 | 0.764 | 0.644 | 0.617 | 0.748 |
| 250 | 1.46 | 1.02 | 2.17 | 0.991 | 2.69 | 0.664 | 0.765 | 0.626 | 0.613 | 0.703 |
| 300 | 1.41 | 0.993 | 2.24 | 0.997 | 2.84 | 0.665 | 0.765 | 0.612 | 0.607 | 0.679 |
| 350 | 1.40 | 0.980 | 2.22 | 0.981 | 2.92 | 0.664 | 0.765 | 0.612 | 0.607 | 0.666 |
| 400 | 1.36 | 0.958 | 2.18 | 0.959 | 2.95 | 0.665 | 0.766 | 0.613 | 0.609 | 0.659 |
| 500 | 1.31 | 0.976 | 2.14 | 0.937 | 2.97 | 0.668 | 0.768 | 0.612 | 0.609 | 0.641 |
| 600 | 1.27 | 0.902 | 2.11 | 0.917 | 2.98 | 0.670 | 0.758 | 0.610 | 0.609 | 0.623 |
| 700 | 1.25 | 0.886 | 2.08 | 0.897 | 2.96 | 0.671 | 0.769 | 0.610 | 0.611 | 0.617 |
| 800 | 1.23 | 0.871 | 2.05 | 0.881 | 2.94 | 0.672 | 0.770 | 0.610 | 0.612 | 0.615 |
| 900 | 1.21 | 0.861 | 2.03 | 0.867 | 2.91 | 0.673 | 0.770 | 0.610 | 0.614 | 0.614 |
| 1000 | 1.20 | 0.851 | 2.01 | 0.856 | 2.89 | 0.674 | 0.770 | 0.610 | 0.615 | 0.613 |

Source: (18:323)

## TABLE 3.3

Regression Calculations For a and b in
$A = aR^b$ (dB/km) as Functions of Frequency
and Dropsize Distribution with Rain Temperature = 0°C

| FREQ. (GHz) | a | | | | | b | | | | |
|---|---|---|---|---|---|---|---|---|---|---|
| | $LP_L$ | $LP_H$ | MP | J-T | J-D | $LP_L$ | $LP_H$ | MP | J-T | J-D |
| 1.0 | $6.41 \times 10^{-5}$ | $5.26 \times 10^{-5}$ | $8.60 \times 10^{-5}$ | $4.71 \times 10^{-5}$ | $8.63 \times 10^{-5}$ | 0.891 | 0.947 | 0.853 | 0.899 | 0.843 |
| 1.5 | $1.45 \times 10^{-4}$ | $1.14 \times 10^{-4}$ | $1.93 \times 10^{-4}$ | $9.31 \times 10^{-5}$ | $1.94 \times 10^{-4}$ | 0.908 | 0.976 | 0.870 | 0.967 | 0.847 |
| 2.0 | $2.61 \times 10^{-4}$ | $1.96 \times 10^{-4}$ | $3.45 \times 10^{-4}$ | $1.36 \times 10^{-4}$ | $3.47 \times 10^{-4}$ | 0.930 | 1.012 | 0.891 | 1.069 | 0.851 |
| 2.5 | $4.16 \times 10^{-4}$ | $2.96 \times 10^{-4}$ | $5.46 \times 10^{-4}$ | $1.63 \times 10^{-4}$ | $5.48 \times 10^{-4}$ | 0.955 | 1.054 | 0.917 | 1.202 | 0.857 |
| 3.0 | $6.15 \times 10^{-4}$ | $4.12 \times 10^{-4}$ | $7.99 \times 10^{-4}$ | $2.09 \times 10^{-4}$ | $8.01 \times 10^{-4}$ | 0.984 | 1.100 | 0.947 | 1.303 | 0.864 |
| 3.5 | $8.67 \times 10^{-4}$ | $5.42 \times 10^{-4}$ | $1.11 \times 10^{-3}$ | $3.08 \times 10^{-4}$ | $1.11 \times 10^{-3}$ | 1.015 | 1.150 | 0.981 | 1.351 | 0.871 |
| 4.0 | $1.16 \times 10^{-3}$ | $6.84 \times 10^{-4}$ | $1.47 \times 10^{-3}$ | $5.08 \times 10^{-4}$ | $1.48 \times 10^{-3}$ | 1.049 | 1.202 | 1.016 | 1.350 | 0.879 |
| 5.0 | $1.94 \times 10^{-3}$ | $1.12 \times 10^{-3}$ | $2.41 \times 10^{-3}$ | $1.38 \times 10^{-3}$ | $2.40 \times 10^{-3}$ | 1.113 | 1.274 | 1.079 | 1.288 | 0.896 |
| 6.0 | $3.05 \times 10^{-3}$ | $1.99 \times 10^{-3}$ | $3.71 \times 10^{-3}$ | $3.06 \times 10^{-3}$ | $3.59 \times 10^{-3}$ | 1.158 | 1.285 | 1.124 | 1.271 | 0.913 |
| 7.0 | $4.55 \times 10^{-3}$ | $3.36 \times 10^{-3}$ | $5.44 \times 10^{-3}$ | $5.57 \times 10^{-3}$ | $5.07 \times 10^{-3}$ | 1.180 | 1.270 | 1.147 | 1.167 | 0.929 |
| 8.0 | $6.49 \times 10^{-3}$ | $5.35 \times 10^{-3}$ | $7.65 \times 10^{-3}$ | $9.07 \times 10^{-3}$ | $6.86 \times 10^{-3}$ | 1.187 | 1.245 | 1.156 | 1.118 | 0.943 |
| 9.0 | $8.88 \times 10^{-3}$ | $8.03 \times 10^{-3}$ | $1.04 \times 10^{-2}$ | $1.29 \times 10^{-2}$ | $8.96 \times 10^{-3}$ | 1.185 | 1.216 | 1.155 | 1.091 | 0.957 |
| 10 | $1.17 \times 10^{-2}$ | $1.14 \times 10^{-2}$ | $1.36 \times 10^{-2}$ | $1.69 \times 10^{-2}$ | $1.14 \times 10^{-2}$ | 1.178 | 1.189 | 1.150 | 1.076 | 0.968 |
| 11 | $1.50 \times 10^{-2}$ | $1.52 \times 10^{-2}$ | $1.73 \times 10^{-2}$ | $2.12 \times 10^{-2}$ | $1.41 \times 10^{-2}$ | 1.171 | 1.167 | 1.143 | 1.065 | 0.977 |
| 12 | $1.86 \times 10^{-2}$ | $1.96 \times 10^{-2}$ | $2.15 \times 10^{-2}$ | $2.62 \times 10^{-2}$ | $1.72 \times 10^{-2}$ | 1.162 | 1.150 | 1.136 | 1.052 | 0.985 |
| 15 | $3.21 \times 10^{-2}$ | $3.47 \times 10^{-2}$ | $3.66 \times 10^{-2}$ | $4.66 \times 10^{-2}$ | $2.62 \times 10^{-2}$ | 1.142 | 1.119 | 1.118 | 1.010 | 1.003 |
| 20 | $6.26 \times 10^{-2}$ | $7.09 \times 10^{-2}$ | $7.19 \times 10^{-2}$ | $9.83 \times 10^{-2}$ | $5.30 \times 10^{-2}$ | 1.119 | 1.083 | 1.097 | 0.946 | 1.020 |
| 25 | 0.105 | 0.132 | 0.121 | 0.173 | $8.61 \times 10^{-2}$ | 1.094 | 1.029 | 1.074 | 0.884 | 1.033 |
| 30 | 0.162 | 0.226 | 0.186 | 0.274 | 0.128 | 1.061 | 0.964 | 1.043 | 0.823 | 1.044 |
| 35 | 0.232 | 0.345 | 0.268 | 0.372 | 0.180 | 1.022 | 0.907 | 1.007 | 0.783 | 1.053 |
| 40 | 0.313 | 0.467 | 0.362 | 0.451 | 0.241 | 0.981 | 0.864 | 0.972 | 0.760 | 1.058 |
| 50 | 0.489 | 0.669 | 0.579 | 0.629 | 0.387 | 0.907 | 0.815 | 0.905 | 0.709 | 1.053 |
| 60 | 0.658 | 0.796 | 0.801 | 0.804 | 0.558 | 0.850 | 0.794 | 0.851 | 0.682 | 1.035 |
| 70 | 0.801 | 0.869 | 1.00 | 0.833 | 0.740 | 0.809 | 0.784 | 0.812 | 0.661 | 1.009 |
| 80 | 0.924 | 0.913 | 1.19 | 0.809 | 0.922 | 0.778 | 0.780 | 0.781 | 0.674 | 0.980 |
| 90 | 1.02 | 0.945 | 1.35 | 0.857 | 1.10 | 0.756 | 0.776 | 0.753 | 0.663 | 0.953 |
| 100 | 1.08 | 0.966 | 1.48 | 0.961 | 1.26 | 0.742 | 0.774 | 0.730 | 0.637 | 0.928 |
| 110 | 1.12 | 0.979 | 1.59 | 1.06 | 1.41 | 0.734 | 0.771 | 0.714 | 0.614 | 0.904 |
| 120 | 1.15 | 0.981 | 1.67 | 1.10 | 1.55 | 0.727 | 0.771 | 0.702 | 0.604 | 0.882 |
| 150 | 1.25 | 0.993 | 1.88 | 1.04 | 1.89 | 0.703 | 0.769 | 0.677 | 0.610 | 0.829 |
| 200 | 1.46 | 1.05 | 2.06 | 1.01 | 2.33 | 0.668 | 0.764 | 0.648 | 0.612 | 0.775 |
| 250 | 1.49 | 1.04 | 2.13 | 0.983 | 2.60 | 0.660 | 0.763 | 0.634 | 0.614 | 0.724 |
| 300 | 1.44 | 1.00 | 2.24 | 0.976 | 2.78 | 0.661 | 0.764 | 0.614 | 0.611 | 0.692 |
| 350 | 1.44 | 0.990 | 2.23 | 0.968 | 2.87 | 0.659 | 0.765 | 0.610 | 0.609 | 0.673 |
| 400 | 1.40 | 0.969 | 2.19 | 0.951 | 2.92 | 0.660 | 0.765 | 0.611 | 0.610 | 0.664 |
| 500 | 1.33 | 0.930 | 2.14 | 0.934 | 2.94 | 0.665 | 0.767 | 0.611 | 0.609 | 0.650 |
| 600 | 1.28 | 0.902 | 2.11 | 0.920 | 2.96 | 0.669 | 0.768 | 0.609 | 0.608 | 0.630 |
| 700 | 1.25 | 0.884 | 2.08 | 0.901 | 2.96 | 0.671 | 0.769 | 0.610 | 0.610 | 0.620 |
| 800 | 1.22 | 0.868 | 2.05 | 0.884 | 2.94 | 0.672 | 0.770 | 0.610 | 0.611 | 0.616 |
| 900 | 1.21 | 0.858 | 2.03 | 0.869 | 2.91 | 0.673 | 0.770 | 0.610 | 0.613 | 0.614 |
| 1000 | 1.19 | 0.850 | 2.00 | 0.856 | 2.99 | 0.674 | 0.771 | 0.610 | 0.615 | 0.612 |

Source: (18:323)

37

## TABLE 3.4

Regression Calculations For a and b in
$A = aR^b$ (dB/km) as Functions of Frequency
and Dropside Distribution with Rain Temperature = -10°C

| FREQ. (GHz) | a | | | | | b | | | | |
|---|---|---|---|---|---|---|---|---|---|---|
| | $LP_L$ | $LP_H$ | HP | J-T | J-D | $LP_L$ | $LP_H$ | HP | J-T | J-D |
| 1.0 | $8.68{\times}10^{-5}$ | $7.13{\times}10^{-5}$ | $1.16{\times}10^{-4}$ | $6.35{\times}10^{-5}$ | $1.17{\times}10^{-4}$ | 0.892 | 0.948 | 0.854 | 0.901 | 0.843 |
| 1.5 | $1.97{\times}10^{-4}$ | $1.55{\times}10^{-4}$ | $2.62{\times}10^{-4}$ | $1.26{\times}10^{-4}$ | $2.63{\times}10^{-4}$ | 0.909 | 0.978 | 0.871 | 0.970 | 0.847 |
| 2.0 | $3.55{\times}10^{-4}$ | $2.67{\times}10^{-4}$ | $4.71{\times}10^{-4}$ | $1.89{\times}10^{-4}$ | $4.72{\times}10^{-4}$ | 0.931 | 1.014 | 0.892 | 1.065 | 0.852 |
| 2.5 | $5.62{\times}10^{-4}$ | $4.04{\times}10^{-4}$ | $7.45{\times}10^{-4}$ | $2.48{\times}10^{-4}$ | $7.47{\times}10^{-4}$ | 0.955 | 1.053 | 0.917 | 1.169 | 0.858 |
| 3.0 | $8.38{\times}10^{-4}$ | $5.68{\times}10^{-4}$ | $1.09{\times}10^{-3}$ | $3.38{\times}10^{-4}$ | $1.09{\times}10^{-3}$ | 0.981 | 1.094 | 0.944 | 1.243 | 0.864 |
| 3.5 | $1.17{\times}10^{-3}$ | $7.57{\times}10^{-4}$ | $1.51{\times}10^{-3}$ | $5.06{\times}10^{-4}$ | $1.51{\times}10^{-3}$ | 1.008 | 1.134 | 0.971 | 1.271 | 0.870 |
| 4.0 | $1.57{\times}10^{-3}$ | $9.80{\times}10^{-4}$ | $2.00{\times}10^{-3}$ | $7.81{\times}10^{-3}$ | $2.00{\times}10^{-3}$ | 1.033 | 1.171 | 0.998 | 1.270 | 0.877 |
| 5.0 | $2.59{\times}10^{-3}$ | $1.82{\times}10^{-3}$ | $3.26{\times}10^{-3}$ | $1.79{\times}10^{-3}$ | $3.22{\times}10^{-3}$ | 1.077 | 1.214 | 1.041 | 1.228 | 0.889 |
| 6.0 | $3.96{\times}10^{-3}$ | $2.64{\times}10^{-3}$ | $4.91{\times}10^{-3}$ | $3.45{\times}10^{-3}$ | $4.76{\times}10^{-3}$ | 1.105 | 1.222 | 1.068 | 1.180 | 0.901 |
| 7.0 | $5.70{\times}10^{-3}$ | $4.14{\times}10^{-3}$ | $6.98{\times}10^{-3}$ | $5.68{\times}10^{-3}$ | $6.63{\times}10^{-3}$ | 1.119 | 1.214 | 1.083 | 1.145 | 0.910 |
| 8.0 | $7.81{\times}10^{-3}$ | $6.07{\times}10^{-3}$ | $5.50{\times}10^{-3}$ | $8.43{\times}10^{-3}$ | $8.82{\times}10^{-3}$ | 1.125 | 1.199 | 1.090 | 1.118 | 0.919 |
| 9.0 | $1.03{\times}10^{-2}$ | $8.46{\times}10^{-3}$ | $1.25{\times}10^{-2}$ | $1.16{\times}10^{-2}$ | $1.14{\times}10^{-2}$ | 1.126 | 1.185 | 1.092 | 1.099 | 0.926 |
| 10 | $1.32{\times}10^{-2}$ | $1.13{\times}10^{-2}$ | $1.59{\times}10^{-2}$ | $1.51{\times}10^{-2}$ | $1.42{\times}10^{-2}$ | 1.125 | 1.171 | 1.092 | 1.087 | 0.932 |
| 11 | $1.64{\times}10^{-2}$ | $1.45{\times}10^{-2}$ | $1.97{\times}10^{-2}$ | $1.91{\times}10^{-2}$ | $1.74{\times}10^{-2}$ | 1.124 | 1.161 | 1.091 | 1.077 | 0.938 |
| 12 | $2.00{\times}10^{-2}$ | $1.81{\times}10^{-2}$ | $2.39{\times}10^{-2}$ | $2.37{\times}10^{-2}$ | $2.09{\times}10^{-2}$ | 1.122 | 1.152 | 1.090 | 1.066 | 0.942 |
| 15 | $3.31{\times}10^{-2}$ | $3.14{\times}10^{-2}$ | $3.94{\times}10^{-2}$ | $4.29{\times}10^{-2}$ | $3.34{\times}10^{-2}$ | 1.119 | 1.135 | 1.088 | 1.027 | 0.954 |
| 20 | $6.37{\times}10^{-2}$ | $6.68{\times}10^{-2}$ | $7.50{\times}10^{-2}$ | $9.73{\times}10^{-2}$ | $6.09{\times}10^{-2}$ | 1.111 | 1.058 | 1.082 | 0.951 | 0.971 |
| 25 | 0.107 | 0.130 | 0.126 | 0.174 | $9.73{\times}10^{-2}$ | 1.091 | 1.037 | 1.065 | 0.887 | 0.988 |
| 30 | 0.165 | 0.226 | 0.193 | 0.276 | 0.143 | 1.059 | 0.969 | 1.037 | 0.826 | 1.004 |
| 35 | 0.236 | 0.346 | 0.275 | 0.376 | 0.197 | 1.021 | 0.910 | 1.002 | 0.784 | 1.016 |
| 40 | 0.316 | 0.468 | 0.370 | 0.455 | 0.260 | 0.981 | 0.867 | 0.968 | 0.761 | 1.025 |
| 50 | 0.487 | 0.665 | 0.579 | 0.619 | 0.404 | 0.910 | 0.818 | 0.904 | 0.714 | 1.027 |
| 60 | 0.645 | 0.789 | 0.787 | 0.800 | 0.564 | 0.856 | 0.796 | 0.854 | 0.664 | 1.016 |
| 70 | 0.777 | 0.860 | 0.973 | 0.840 | 0.728 | 0.817 | 0.785 | 0.817 | 0.659 | 0.997 |
| 80 | 0.888 | 0.903 | 1.14 | 0.808 | 0.888 | 0.787 | 0.781 | 0.789 | 0.673 | 0.974 |
| 90 | 0.980 | 0.935 | 1.25 | 0.834 | 1.04 | 0.765 | 0.777 | 0.764 | 0.668 | 0.953 |
| 100 | 1.05 | 0.957 | 1.41 | 0.920 | 1.18 | 0.749 | 0.774 | 0.741 | 0.646 | 0.933 |
| 110 | 1.09 | 0.974 | 1.51 | 1.01 | 1.32 | 0.739 | 0.771 | 0.724 | 0.624 | 0.914 |
| 120 | 1.12 | 0.980 | 1.59 | 1.06 | 1.44 | 0.733 | 0.770 | 0.712 | 0.611 | 0.896 |
| 150 | 1.20 | 0.979 | 1.80 | 1.05 | 1.76 | 0.711 | 0.769 | 0.686 | 0.610 | 0.846 |
| 200 | 1.42 | 1.03 | 2.04 | 1.02 | 2.21 | 0.674 | 0.765 | 0.652 | 0.609 | 0.754 |
| 250 | 1.50 | 1.04 | 2.11 | 1.01 | 2.53 | 0.659 | 0.763 | 0.638 | 0.608 | 0.739 |
| 300 | 1.45 | 1.01 | 2.22 | 0.972 | 2.72 | 0.660 | 0.764 | 0.618 | 0.612 | 0.704 |
| 350 | 1.45 | 0.994 | 2.23 | 0.963 | 2.82 | 0.658 | 0.764 | 0.612 | 0.610 | 0.684 |
| 400 | 1.42 | 0.976 | 2.19 | 0.942 | 2.88 | 0.658 | 0.765 | 0.611 | 0.612 | 0.669 |
| 500 | 1.34 | 0.936 | 2.14 | 0.927 | 2.91 | 0.664 | 0.767 | 0.611 | 0.611 | 0.655 |
| 600 | 1.29 | 0.904 | 2.11 | 0.919 | 2.94 | 0.668 | 0.768 | 0.608 | 0.609 | 0.634 |
| 700 | 1.25 | 0.883 | 2.08 | 0.903 | 2.95 | 0.671 | 0.769 | 0.609 | 0.609 | 0.622 |
| 800 | 1.22 | 0.869 | 2.05 | 0.886 | 2.93 | 0.672 | 0.770 | 0.610 | 0.611 | 0.617 |
| 900 | 1.21 | 0.857 | 2.03 | 0.871 | 2.91 | 0.673 | 0.770 | 0.610 | 0.613 | 0.614 |
| 1000 | 1.19 | 0.849 | 2.00 | 0.857 | 2.89 | 0.674 | 0.771 | 0.611 | 0.614 | 0.613 |

Source: (18:324)

38

Lin (15:557-81) regarding the behavior of rain attenuation.
Lin gathered 31 sets of experimental data on the statistics
of microwave rain attenuation at frequencies above 10 GHz in
the U.S., England, Japan, Italy, and Canada and proposed many
ideas dealing with the statistical behavior of rain attenua-
tion.

The summary of his findings are as follows:

1. the distribution of rain attenuation, a(t), in dB
is approximately lognormal within the attenuation range of
1-50 dB.

2. the distribution of the fade duration, f(A), is also
approximately lognormal.

Lin's theory on the lognormal behavior of rain attenua-
tion suggests that three parameters which depend on geographic
locations determine the distribution of the rain attenuation.
These three parameters are:

$P_o$ = probability of rainfall, the expected fraction of
time that rain falls at the location of the satel-
lite earth station

$\sigma_a$ = standard deviation of the attenuation, $\alpha(t)$

$\alpha_m$ = median of the attenuation, $\alpha(t)$

Lin also stated that $\alpha_m$ is frequency dependent and increases
almost linearly with the path length because the median rain
is usually small and almost uniform over the entire path. $\sigma_a$
decreases slightly as frequency increases and decreases
slightly as the path length increases because of the aver-
aging effect of the propagation volume.

39

The equation describing the lognormal distribution of rain attenuation is

$$P(\alpha > A) = 0.5(P_o)(0.5 + Q[(\log_{10}A - \mu_m)/(2^{0.5}\sigma_a)]) \qquad (3.3)$$

where

$P_o$ = probability of rainfall

$\sigma_a$ = standard deviation of $\log_{10} a$ during the raining time

$\mu_a = \log_{10}\alpha_m$

= mean value of $\log_{10}\alpha$ during the raining time

Similarly, the distribution of the fade, $f(A)$, is described by

$$P(f(a) > b) = 0.5(0.5 + Q[(\log_{10}b - \mu_f)/2^{0.5}\sigma_f)]) \qquad (3.4)$$

where

$\mu_f$ = mean of $\log_{10} f(A)$

$\sigma_f$ = standard deviation of $\log_{10}[f(A)]$

Due to the significance of rain attenuation to the satellite communications systems designer, an ideal method that would permit an accurate extrapolation of measured rain characteristics to different geographical locations or other time periods is needed. Since detailed measurements of the various important statistics of rainfall exist for only a few locations throughout the world, it would be of great value if these statistics could be accurately applied or converted to other areas, especially those with different climates. However, a

good deterministic theory of rain generation and rainfall

has not been developed, therefore it is not possible to

apply it to the prediction of localized rain occurrences.

## IV. Diversity Techniques For Satellite Communications

With the recent growth of satellite communications, allocations in the higher frequency bands have been required to relieve the congestion in the 8/7 GHz band. One such allocation is the 30/20 GHz band, which is being considered for many government applications (9:1-1). Unfortunately, a severe problem with rain attenuation exists in the 30/20 GHz frequency band (as noted in Sections II and III).

There are many techniques that can be employed to overcome the rain attenuation. In order to overcome the deep fades on the uplink or downlink, satellite transmitters could employ higher power levels or the associated earth station could use a larger antenna (1:369). However, another concept used to combat the effects of rain attenuation is diversity, which is employed to reduce the margin required for rain attenuation. The main concept of diversity is that the probability of an error can be reduced by using two or more received signals to determine the actual transmitted signal instead of one.

### Description of Basic Diversity System

There are three basic types of diversity: angle, frequency, and space (or site). The use of angle diversity requires two or more satellites which are separated physically such that the fading on any earth-space path has a low correlation with the fading on other paths (9:3-1)

(See Figure 4.1). Due to the requirement for two satellites, angle diversity is very costly and it has been shown to be not as effective as the other two diversity methods (9:1-2). Frequency diversity requires that the satellite be equipped with two transponders, one operating in a high frequency band and the other in a lower band. When the rain attenuation is minimal the higher band is used and the lower frequency band transponder is used when the rain attenuation becomes significant. Although the fades in the two bands are correlated, the fade depths in the lower frequency band are less than the higher frequency band. Frequency diversity incurs a relatively high cost for the additional satellite transponder but the performance has been rated the highest of the three diversity methods (9:1-2).

However, the focus of this thesis effort is on space diversity techniques that can be used to combat rain attenuation in the downlink of a satellite communications link. The use of site diversity in the downlink requires that two or more earth terminals be physically separated such that the fading on any space-earth path has a low correlation with the fading on other paths (9:2-1). Dual diversity is the most basic type of space diversity but higher orders of diversity may be needed at locations with a history of heavy rains. However, the higher the order of diversity, the more costly the system due to the additional earth stations.

A block diagram of a dual downlink space diversity system is shown in Figure 4.2. Since the diversity equipment
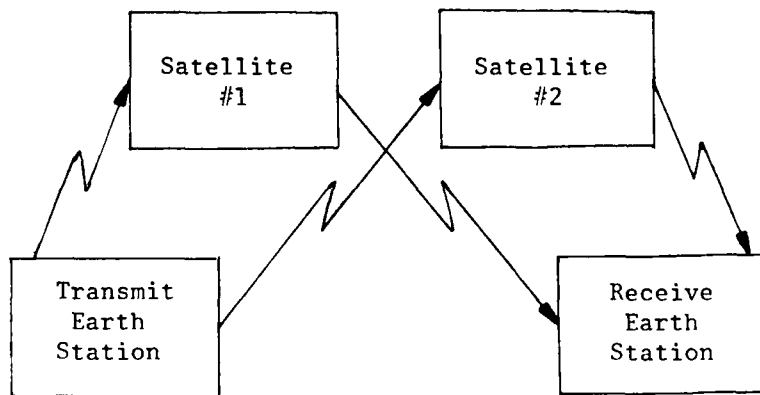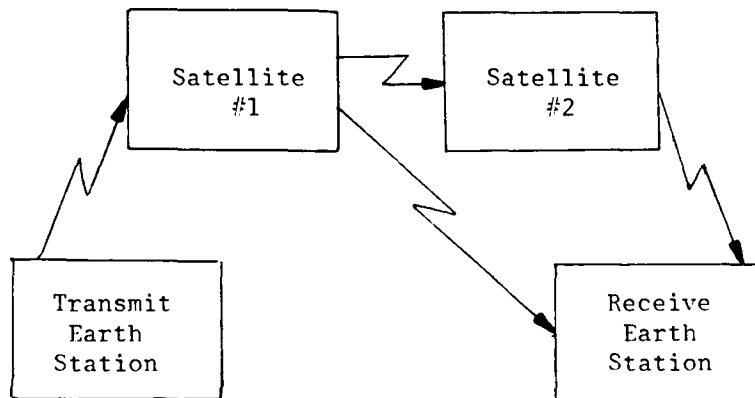
Figure 4.1a  Without Intersatellite Links

Figure 4.1b  With Intersatellite Links
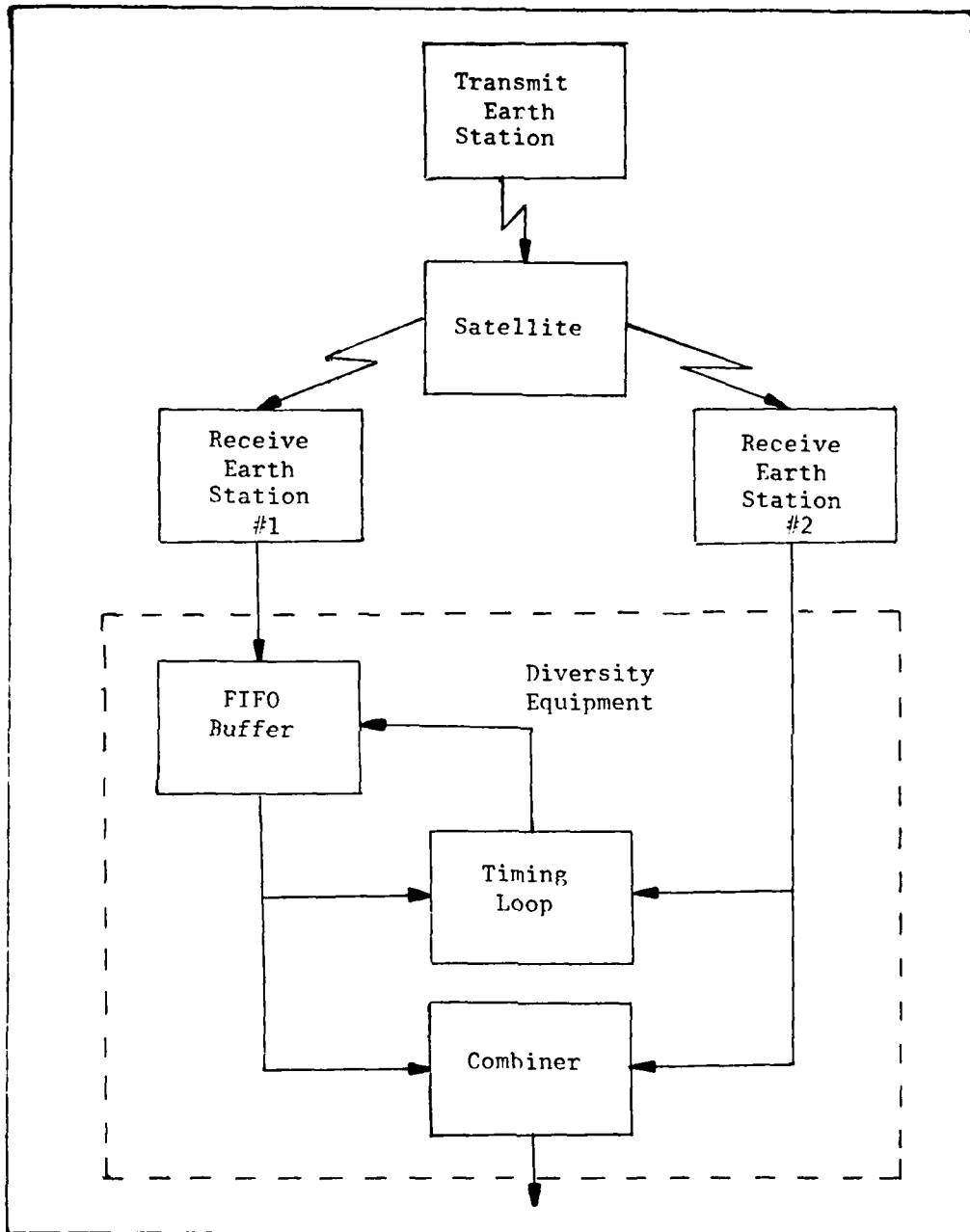
Figure 4.1   Angle Diversity

Source: (9:3-2)

44

Figure 4.2   Block Diagram--Downlink Space Diversity

combines the digital outputs of the two earth stations, the
configuration is independent of whether Frequency Division
Multiple Access (FDMA) or Time Division Multiple Access (TDMA)
is used on the satellite communications link (9:2-1). The
diversity equipment could be collocated with one of the
earth stations or it could be located at a separate site.

The optimum spacing between the earth stations is
dependent on the characteristics of the rain in that partic-
ular area. In practice, optimum spacing may not be achiev-
able because of limitations on the availability of sites for
earth stations. However, the spacing will usually be in
excess of one mile necessitating the use of a terrestrial
link to connect at least one earth station to the diversity
equipment.

Bit Stream Synchronization. When using diversity on the
downlink, there will usually be a difference in the transmis-
sion path lengths from the satellite to the combiner. How-
ever, due to the satellite motion, this difference in path
lengths will not remain constant. The path length difference
and its variation are functions of the relative geographical
locations of the earth stations and the satellite (9:2-3).
Therefore, due to the path length difference, some adjustment
or control must be made to maintain bit synchronization of
the bit streams into the combiner. If the path length dif-
ference is a significant fraction of a bit, a common prac-
tice is to use a first-in-first-out (FIFO) buffer on the
shorter path as shown in Figure 4.2 so that the bits arrive

46

at the combiner in synchronism (9:2-5). If the variation in the path length difference is a significant fraction of a bit, a timing tracking loop is needed to maintain synchronism. In many cases, this loop operates similarly to the code tracking loop in a pseudonoise receiver except that one of the two bit streams is used as a reference (9:2-5).

Linear Diversity Combining Techniques. When using spatial diversity a combining technique must be used to choose the optimum signal from the diversity branches. The most common methods for combining diversity channels outputs are:

1. Selection combining. Selection of the channel with the highest signal level. Measurement of the signal level is required and this method can use either hard or soft decisions.

2. Maximum Selection combining. Selection of the received symbol with the largest amplitude. The method requires soft-decision outputs.

3. Equal Gain. Summing the soft-decision outputs of each channel.

4. Square Law combining. Squaring the soft-decision output of each channel followed by linear summing.

5. Maximum Ratio combining. Weighting the soft-decision output of each channel by the SNR. The measurement of the SNR is required.

The diversity improvement is dependent on many factors including the rain fading characteristics of that particular

area (1:369). However, theoretically, maximum ratio com-
bining is the most efficient, and selection combining is the
least (9:2-8). Since the difference in performance between
the different combining methods is relatively small, the
decision of which method to use can vary with the particular
implementation depending on the desired performance criteria
and cost restrictions.

## Space Diversity Measurements

The rain attenuation effects on the transmitted signal
for a slant-path link can be measured directly, or inferred
from the measurement of other related parameters by using
one of the following techniques (1:369-70):

1. direct reception of a beacon signal transmitted
from a geostationary satellite at the required frequency.

2. radiometric measurements using either the sun as a
source or the apparent change in sky temperature with rain-
fall intensity.

3. rapid-response raingauges.

4. radar.

As noted in Table 4.1, there are advantages and limita-
tions for each of the different measurement techniques for
obtaining slant-path attenuation. The three major advantages
of the radiometer are relative cheapness, extreme reliability
and straightforward data reduction. For gathering long-term
data for slant-path attenuation, the most cost-effective
solution is the radiometer (1:370). Fast-response raingauges,

48

TABLE 4.1

Measurement Techniques For Obtaining Slant-Path Attenuation

| Technique | Relative cost | Elevation angles sampled | Accuracy in calculating attenuation | Comments |
|---|---|---|---|---|
| (a) Satellite beacon measurements | extremely expensive satellite moderately expensive earth stations | fixed | excellent fade margins > 30dB | limited to satellite lifetime |
| (b) Radiometers (i) sun tracking | moderately cheap | varies with sun | good to 20dB | limited operating hours and elevation angles |
| (ii) sky-noise Dicke switching | moderately cheap | fixed | good to 13dB | possibly limited to frequencies $\leqslant$ 30GHz |
| (iii) sky-noise total power | cheap | fixed | good to 10dB | |
| (c) Raingauges | very cheap | any | generally poor | highly dependent on wind and rain-drop parameters |
| (d) Radar | moderate to very expensive | any | variable | highly dependent on physical phase of scattering particles |

Source:(1:370)

49

although inexpensive, do not provide data that can be easily transformed into slant-path attenuation data. In order to provide an accurate transformation of collected data into slant-path attenuation data, an extensive array of rain-gauges, accurate telemetry and large computing facilities are required, which greatly increases the associated costs of this measurement technique. Radar is a very useful tool for investigating propagation phenomena; however, there are also some potential problem areas. Unless great care is used in eliminating all echoes due to solid or solid/liquid phase particles, very large errors will accrue in the calculation of the slant-path attenuation (1:370). The best measurement method for obtaining the desired slant-path propagation data is the satellite beacon technique. However, to orbit radio beacons covering a vast range of frequencies is extremely expensive thus the opportunity of conducting satellite-beacon propagation experiments rarely exists except for a limited period at a few frequencies and locations (1:370).

Diversity Performance Assessment Techniques

There are two major methods currently employed in assessing the performance of space diversity systems: diversity gain and diversity improvement. Diversity gain is defined as the difference between the path attenuation associated with a single earth station and the diversity modes of operation for a given percentage time (13:280). It uses (percentage of) the time as a parameter and expresses the diversity

improvement as the difference in decibels which is the effec-
tive increase in fade margin between the single earth sta-
tion site and the diversity system fading statistics. Diver-
sity improvement is defined as the ratio of the percentage
time a given fade depth is exceeded on a single path to the
percentage time that the same fade depth is exceeded for the
diversity system (13:280). An example of these two perform-
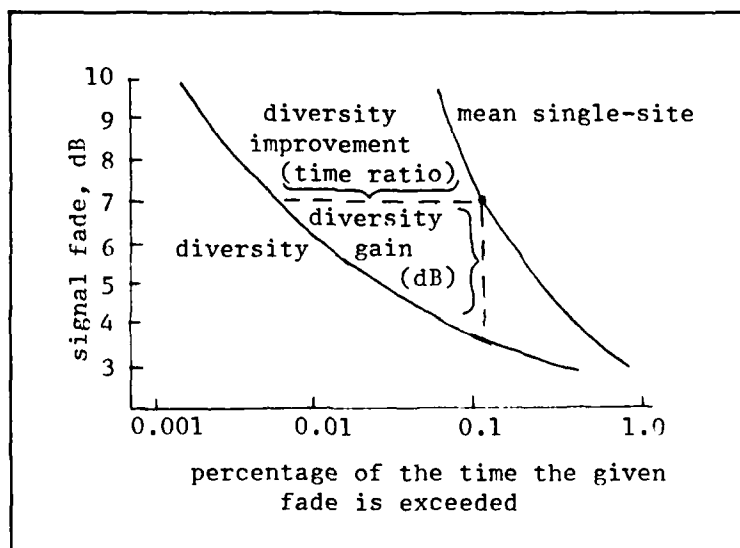ance measures is depicted in Figure 4.3.



Figure 4.3   Technique for Calculating Diversity
             Improvement and Diversity Gain from
             Single-Site and Space Diversity
             Cumulative Fading Statistics.

Although the methods for describing diversity perform-
ance are identical, some space diversity experiments have
shown that the diversity gain technique exhibits a more con-
sistent behavior than the diversity improvement technique
when different sets of propagation data are compared. This

51

observation is probably due to the fact that the calculation of the improvement factor involves division by a percentage time which is often very small and therefore subject to considerable uncertainty (13:281). Since diversity gain is a function of the single earth station site fading depth characteristics, it is commonly used to compare sets of space-diversity measurements conducted over different periods of time and during different weather conditions. Hence, the diversity gain method of performance measurement for diversity systems is generally preferred to the diversity improvement method.

Much research has been conducted to develop a model which accurately predicts the performance of a diversity system with respect only to the separation distances between the earth stations and not to the carrier frequency (1,13). One of the best known models of this type is the empirical relationship for path diversity gain developed by D.B. Hodge in the mid-70's (13:280-1). Hodge gathered diversity gain data for millimeter wavelength earth-space propagation paths in Ohio and New Jersey. Although these measurements were collected in different locations and over different time periods, the resulting diversity gain data were very consistent. Hodge used this to develop an empirical relationship for diversity gain as a function of separation distance and single earth station fade depth. He recognized that the diversity gain data followed the same relationship for each

value of the single earth station fade depth. This relationship for diversity gain, $G_d$, is

$$G_d = a(1 - \exp(-bD)) \tag{4.1}$$

where

a = A - 3.6(1 - exp(-0.24A))

b = 0.46(1 - exp(-0.26A))

A = single earth station fade depth in dB

D = earth station separation distance in km

The coefficients a and b depend only upon the single earth station fade depth and were found by performing a minimum rms error fit for each fade depth.

Although Hodge's relationship for diversity gain accurately modeled the data measurements collected for his experiment, there have been other similar experiments where the collected data were not accurately modeled by the Hodge relation. Fimbel and Juy assumed that diversity gain was frequency dependent and recalculated the coefficients a and b from Hodge's formula and were able to develop a relationship that more accurately predicted the results of the data measurements that they had collected in the United Kingdom (1:374).

In an effort to improve its accuracy, Hodge later modified his model for diversity gain as a function of earth terminal separation distance, link frequency, elevation angle, and angle between the baseline and the path azimuth (12:1393-9). His new model for diversity gain, $G_D$, is

$$G_D = G_d G_f G_e G_b \qquad (4.2)$$

where

$G_d$ = function defined by Eq (4.1)

$G_f$ = function of frequency

$G_e$ = function of elevation angle

$G_b$ = function of orientation of the baseline relative to the propagation path

$$G_f = 1.64 \exp(-0.025f) \qquad (4.3)$$

where f = link frequency in gigahertz

$$G_e = 0.00492e + 0.834 \qquad (4.4)$$

where e = elevation angle

$$G_b = 0.00177b + 0.887 \qquad (4.5)$$

where b = orientation of the baseline relative to the propagation path in degrees

A set of thirty-four experiments were conducted to validate the Hodge's improved diversity model and the model reproduced the original data set with a rms error of 0.73 dB.

The research in this area has continued but so far no single model developed has been able to accurately predict all of the diversity gain data measurements gathered by experiments conducted throughout the world. It is widely believed that the difficulty in establishing a general model for predicting the diversity gain with respect to separation

distance is that there are several causes of variation for the diversity gain data measurements. The three basic categories which cause diversity gain variation are climatic, geographic, and systemic (1:372).

The climatic factors which cause variations in diversity gain are associated with large scale weather patterns. They are rain lifetimes, rain cell sizes, rain cell separation, and rain cell orientation. In different locations or during different periods, these climatic factors may vary and cause a variation in the diversity gain measurements with respect to earth station separation distances.

The geographic causes relate to the fact that there can be local variations in climate within a limited area as small as 10 km. The geographic feature that seem to enhance or reduce the rainfall-intensity probability at given locations is generally referred to as the microclimate of a region (1:373). These local variations in climate are of particular importance for space diversity communications systems since knowledge of where the high and low probability areas of intense rainfall would greatly aid in the siting of earth stations.

The systemic causes of variations in diversity gain measurements are variation with frequency, variation with elevation angle, variation with baseline orientation, and variation with site separation. The first three variations deal with the concept that rain attenuation varies with frequency and the slant-path of the rain with respect to the

earth station. The fourth variation, separation distance, deals with the fact that a good site location is dependent on several factors, including the microclimate, prevailing wind direction, and the viewing bearing. Thus, the separation distance is dictated by the results of these other factors. However, site separations of approximately 10 km seem to provide diversity gain close to the optimum although some regions will require larger separation distances to achieve the same diversity gain because of geographic and climatic reasons (1:374).

## V. Analysis of Selected Linear Diversity Combining Techniques

In the previous section, it was mentioned that a diversity combining technique must be implemented within the diversity network in order to successfully achieve spatial diversity improvements. In this section, some of the diversity combining techniques will be examined so that a probability of bit error analysis can be performed on the selected combinations of diversity techniques and digital signaling schemes. The diversity techniques to be examined are the selection diversity, equal gain, and maximal ratio techniques and the digital signal-schemes are restricted to DQPSK and B-ary PSK. Therefore, the possible combinations of these diversity techniques and signaling schemes will result in six different probability of bit error expressions.

## Considerations for Bit Error Analysis

In performing such an analysis, there are assumptions that must be stated in order to validate the analysis. Some of the assumptions for the development of the statistics for the two digital signaling schemes are:

1. The channel through which the signaling waveforms are transmitted is assumed to have no bandwidth restrictions (i.e., the ideal case).

2. The signals transmitted through the channel are corrupted by additive white gaussian noise (AWGN).

3.  The receivers at the earth stations are synchro-nized to the satellite transmitter.

4.  The carrier phase is known perfectly at the receiver in order to facilitate ideal coherent demodulation.

5.  All of the lowpass signal representations in each particular signaling scheme have the same energy and are equiprobable.

The diversity/signaling scheme combinations will be compared on the basis of average bit error rate, $P_B$.  If

$$P_B(\gamma_b) = \text{conditional probability of bit error given } \gamma_b \text{ for a specified signaling scheme}$$

$$p_D(\gamma_b) = \text{probability of density function of } \gamma_b \text{ for a particular diversity combining technique}$$

then [as in Eq 7.4.14 from (Ref 19:474)]

$$P_B = \int_0^\infty P_B(\gamma_b) p_D(\gamma_b) d\gamma_b \qquad (5.1)$$

Consider first DQPSK, Referring to Section II Eq (2.30) of this thesis

$$P_B, DQPSK(\gamma_b) = Q(a,b) - 0.5 I_0(a,b) \exp\left[-0.5(a^2 + b^2)\right]$$

where

$$a = 1.0824 \ (0.5\gamma_b)^{0.5}$$

$$b = 2.6131 \ (0.5\gamma_b)^{0.5}$$

$$Q(a,b) = \exp(-0.5(a^2 + b^2)) \sum_{K=0}^\infty \left(\frac{a}{b}\right)^K I_K(ab), \text{ for } b > a > 0$$

58

A further simplification is provided by Shanmugam
(21:425).  For 4-ary DPSK

$$P_{B,DQPSK}(\gamma_b) \approx 2Q[(4\gamma_b \sin^2(\pi/8))^{0.5}] \qquad (5.2)$$

For M-ary PSK signaling the probability of a symbol
error is expressed by

$$P_M = 1 - \int_{\frac{-\pi}{M}}^{\frac{\pi}{M}} \cdot p(\theta)d\theta \qquad (5.3)$$

where

$$p(\theta) = \frac{1}{2\pi} \exp(-\gamma_b)[1+(4\pi\gamma_b)^{0.5}(\frac{\cos\theta}{(2\pi)^{0.5}})$$

$$\cdot \exp(\gamma_b \cos^2\theta) \int_{-\infty}^{(2\gamma_b \cos\theta)^{0.5}} \exp(-0.5x^2)dx]$$

The probability of a bit error for an 8-ary PSK system
with Gray code assignment of 3-tuples (Figure 5.1) can be
expressed by

$$P_{B,8PSK}(\gamma_b) = \sum_{K=1}^{3} (K \text{ errors}) (P_{eK}) \qquad (5.4)$$

where

$P_{eK}$ = probability of error for K bit errors
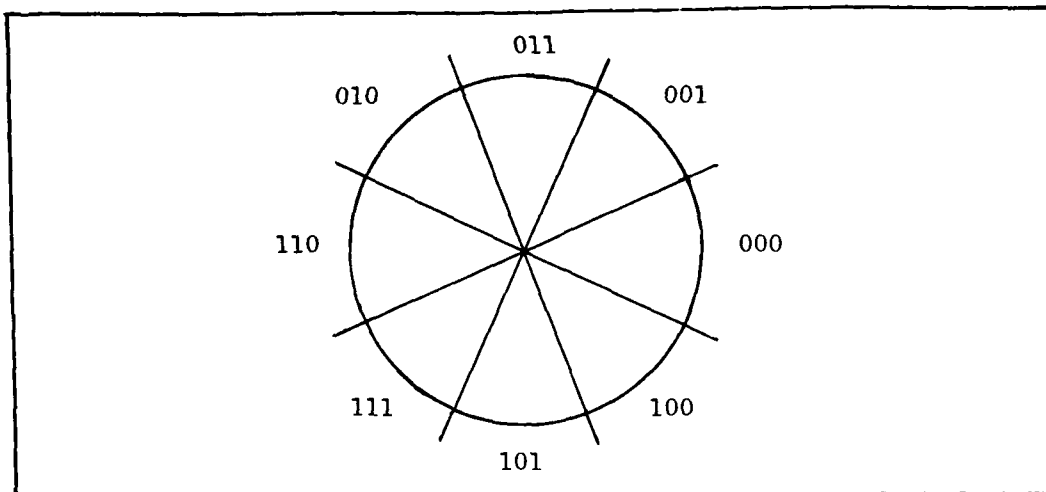
Figure 5.1    Gray Code for 8-ary PSK

Therefore,

$$
P_{B, 8PSK}(\gamma_b) = \left[ \int_{\pi/8}^{3\pi/8} p(\theta)d\theta + 2 \int_{3\pi/8}^{5\pi/8} p(\theta)d\theta + \int_{5\pi/8}^{7\pi/8} p(\theta)d\theta \right.
$$

$$
+ 2 \int_{7\pi/8}^{9\pi/8} p(\theta)d\theta + 3 \int_{9\pi/8}^{11\pi/8} p(\theta)d\theta + 2 \int_{11\pi/8}^{13\pi/8} p(\theta)d\theta
$$

$$
+ \int_{13\pi/8}^{15\pi/8} p(\theta)d\theta \qquad\qquad (5.5)
$$

Since $p(\theta)$ is an even function, Eq (5.5) reduces to

$$
P_{B, 8PSK}(\gamma_b) = 2 \int_{\pi/8}^{3\pi/8} p(\theta)d\theta + 4 \int_{3\pi/8}^{5\pi/8} p(\theta)d\theta + 4 \int_{5\pi/8}^{7\pi/8} p(\theta)d\theta
$$

$$
+ \int_{7\pi/8}^{\pi} p(\theta)d\theta \qquad\qquad (5.6)
$$

60

Due to the complexity of evaluating the substitution of Eq (5.3) into Eq (5.6), the approximation denoted by Eq (2.28) is commonly used for the probability of bit error for high order M-ary PSK systems. For 8-ary PSK

$$P_{B,8PSK}(\gamma_b) \approx \frac{2}{3} Q[(6\gamma_b)^{0.5}\sin(\pi/8)] \qquad (5.7)$$

## Assumptions for Diversity Analysis

Having developed the probability of bit error for each signaling scheme, we must now look at the different linear diversity techniques. Since the digital signaling techniques being used require coherency, we will limit the diversity techniques to those which are most commonly used with coherent signaling schemes. These three diversity techniques, selection, equal gain, and maximal ratio, can all be generally described by the equation

$$f(t) = a_1f_1(t) + \ldots + a_Lf_L(t) = a_jf_j(t) \qquad (5.8)$$

where

$f(t)$ = selected output of diversity system

$a_j$ = combining coefficient proportional to the gain of the jth channel

$f_j$ = received signal of the jth channel

$L$ = number of diversity channels

There are several assumptions about the channel characteristics that must be stated before attempting further development. The basic assumptions are made for the channels when employing the selected linear diversity techniques are:

61

1.  The channel impulse response will be modeled as a zero mean complex-valued gaussian process so that its envelope at any time, t, is Rayleigh-distributed.

2.  The amplitude variations in the received signal, i.e., signal fading, are caused by the time-variant multipath channel characteristics. Due to assumption 1, the channel attenuation, $\alpha$, is Rayleigh-distributed; therefore $\alpha^2$ has a chi-square probability distribution with 2 degrees of freedom. Since $E_b$ is dependent on $\alpha^2$, $\gamma_b$ is also chi-square-distributed.

3.  The information-bearing signal transmitted through the channel is large in comparison to the bandwidth of the transmitted signal so that the channel is considered frequency-nonselective.

4.  The signal bandwidth and the signaling interval shall be chosen small enough so that the channel attenuation and phase shift are essentially fixed for the duration of at least one signaling interval; therefore the channel can be considered slowly fading.

5.  The channel fading is sufficiently slow so that the phase shift can be perfectly estimated from the received signal.

6.  The noise in each channel is independent of the signal and additive; and the received signal, $f_j(t) = s_j(t) + n_j(t)$, where $s_j$ and $n_j$ are the signal and noise components, respectively, in the jth channel.

7.  The noise components, $n_j(t)$ are locally uncorrelated and have zero means.

## Probability of Error in Rayleigh Channel with No Diversity

In order to evaluate the benefits of a diversity system, the probability of a bit error must be calculated for DQPSK and 8-ary PSK in a frequency-nonselective, slowly Rayleigh fading channel without diversity using the same assumptions about the channels as for the diversity case. By assumption 2, $\gamma_b$ is chi-square distributed, therefore,

$$P_{\text{no diversity}}(\gamma_b) = \frac{1}{\overline{\gamma}_b} \exp\left(-\gamma_b/\overline{\gamma}_b\right) \tag{5.9}$$

Using Eq (5.1), the probability of a bit error can be obtained for DQPSK and 8-ary PSK in a Rayleigh channel without diversity.

For DQPSK,

$$P_B(\text{DQPSK, no diversity}) = \int_o^\infty \frac{1}{\overline{\gamma}_b} \exp\left(-\gamma_b/\overline{\gamma}_b\right)$$

$$\cdot P_{B,\text{DQPSK}}(\overline{\gamma}_b) d\gamma_b \tag{5.10}$$

where

$$P_{B,\text{DQPSK}}(\gamma_b) = 2Q\left[4\gamma_b\sin^2(\pi/8))^{0.5}\right]$$

For 8-ary PSK,

$$P_B(\text{8PSK, no diversity}) = \int_o^\infty \frac{1}{\overline{\gamma}_b} \cdot \exp(-\gamma_b/\overline{\gamma}_b)$$

$$\cdot P_{B,\text{8PSK}}(\gamma_b) d\gamma_b \tag{5.11}$$

63

where

$$P_{B,8PSK}(\gamma_b) = \frac{2}{3} Q[(6\gamma_b)^{0.5} \sin(\pi/8)]$$

## Selection Diversity

The basic principle of the selection diversity technique is that at any given time, the system picks out the best of the L noisy signals $f_1$, $f_2$, ... , $f_L$, and uses that one alone; and the other signals do not contribute to f(t) (3:1081). The ideal selection diversity combiner is defined as choosing for the system output, during each "instant" of time, the signal from that receiver which has the largest SNR (See Figure 5.2). Therefore, the parameter used to determine the optimum diversity channel is received SNR. If K denotes the index of a channel for which $E_{bK} > E_{bj}$, $j = 1,2, ... L$; where $j = K$, then this type of system can be characterized by the Eq (5.8) where

$$a_j = \begin{array}{l} 1, \text{ for } j = K \\ 0, \text{ for } j = K \end{array} \qquad (5.12)$$

Several methods can be employed for selecting the optimum diversity channel signal. One of the easiest is if all the receivers have the same noise level then the channel with highest total instantaneous power is selected.

## Analysis of Selection Diversity

Given the assumption of short-term fading, the performance of selection diversity can be obtained from the
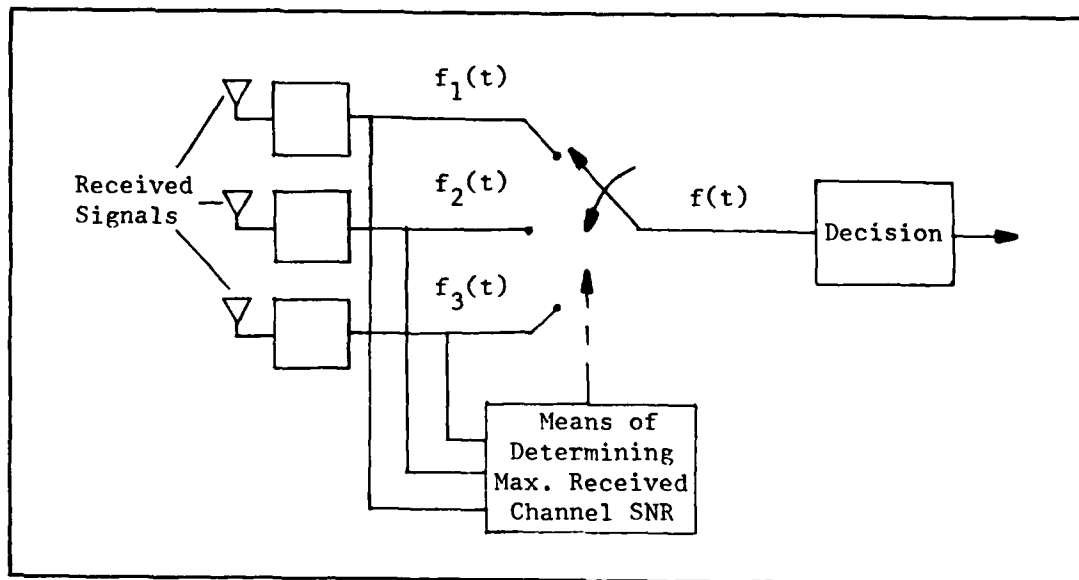
Figure 5.2   Selection Diversity

statistics of the SNR at the selector output.  In partic-
ular, the p.d.f. of $\gamma_{bK}$, the instantaneous SNR in the Kth
channel is needed.  Following the development of Schwartz,
et al., (20:434-5), $P_D(\gamma_{bK})$, can be easily obtained.  Assum-
ing Rayleigh fading and defining $\bar{\gamma}_{cK}$ as the average of $\gamma_b$
over the short-term fading for the Kth channel so that

$$\bar{\gamma}_{cK} = E\{\gamma_{cK}\} = \frac{E\{\alpha_K^2\} \, \mathcal{E}}{N_K} \qquad (5.13)$$

where

   $\alpha_K$ = attenuation factor of Kth channel

   $\mathcal{E}$ = energy of signal transmitted

   $N_K$ = power spectral density of Kth channel

65

yields the individual p.d.f.'s

$$P_D(\gamma_{bK}) = \frac{1}{\bar{\gamma}_{cK}} \exp(-\gamma_{bK}/\bar{\gamma}_{cK}) \tag{5.14}$$

and the associated cumulative distributions are

$$P(\gamma_{bK} < X) = 1 - \exp(-X/\bar{\gamma}_{cK}) \tag{5.15}$$

Over short-term fading, all the events in which the selector output SNR, $\gamma_b$, is less than X is exactly the set of events in which each of the channel SNR's is simultaneously below X (20:435). Since the fading is assumed independent in each of the L channels, the probability that $\gamma_b < X$ is the product of the independent probabilities that each $\gamma_{bK} < X$.

Therefore,

$$P(\gamma_b < X) = \prod_{K=1}^{L} P(\gamma_{bK} < X) = \prod_{K=1}^{L} [1 - \exp(-X/\bar{\gamma}_{cK})] \tag{5.16}$$

The corresponding p.d.f. for $\gamma_b$ is

$$P_D(\gamma_b) = \frac{d}{dX} \left\{ \prod_{K=1}^{L} [1 - \exp(-X/\bar{\gamma}_{cK})] \right\} \; X = \gamma_b \tag{5.17}$$

$$= \frac{d}{d\gamma_b} \left\{ \prod_{K=1}^{L} [1 - \exp(-\gamma_b/\bar{\gamma}_{cK})] \right\} \tag{5.18}$$

If we assume all diversity channels have equal mean SNR over the short-term fading, $\bar{\gamma}_{cK} = \tilde{\gamma}_c$ ; then

$$P(\gamma_b < X) = [1 - \exp(-X/\bar{\gamma}_c)]^L \qquad (5.19)$$

$$p_D(\gamma_b) = \frac{L}{\bar{\gamma}_c} \exp\left(-\gamma_b/\bar{\gamma}_c\right)[1-\exp(-\gamma_b/\bar{\gamma}_c)]^{L-1} \qquad (5.20)$$

Now the probability of bit error can be calculated for the selection diversity combining technique using DQPSK and 8-ary PSK.

For selection diversity using DQPSK,

$$P_B(\text{DQPSK, selection diversity}) = \int_0^\infty \frac{L}{\bar{\gamma}_c} \exp\left(-\gamma_b/\bar{\gamma}_c\right)$$

$$\cdot [1-\exp(-\gamma_b/\bar{\gamma}_c)]^{L-1}$$

$$\cdot P_{B,\text{DQPSK}}(\gamma_b) d\gamma_b \quad (5.21)$$

where

$$P_{B,\text{DQPSK}}(\gamma_b) = 2Q[(4\gamma_b \sin^2(\pi/8))^{0.5}]$$

For selection diversity using 8-ary PSK,

$$P_B(\text{8PSK, selection diversity}) = \int_0^\infty \frac{L}{\bar{\gamma}_c} \exp\left(-\gamma_b/\bar{\gamma}_c\right)$$

$$\cdot [1-\exp(-\gamma_b/\bar{\gamma}_c)]^{L-1}$$

$$\cdot P_{B,\text{8PSK}}(\gamma_b) d\gamma_b \quad (5.22)$$

where

$$P_{B,\text{8PSK}}(\gamma_b) = \frac{2}{3} Q[(6\gamma_b)^{0.5}\sin(\pi/8)]$$

## Equal Gain Diversity

This diversity technique is characterized by the property that all channels have exactly the same gain (3:1081). In terms of Eq (5.8)

$$a_j = 1, \quad j = 1,2, \ldots, L \qquad (5.23)$$

The principle of this method is that all the received channel signals, $f_j(t)$, are added together and the resulting $f(t)$ is formed (See Figure 5.3). The parameter for choosing the optimum signal is a summation of the signals (i.e., signal strengths) to determine which symbol signal was transmitted.
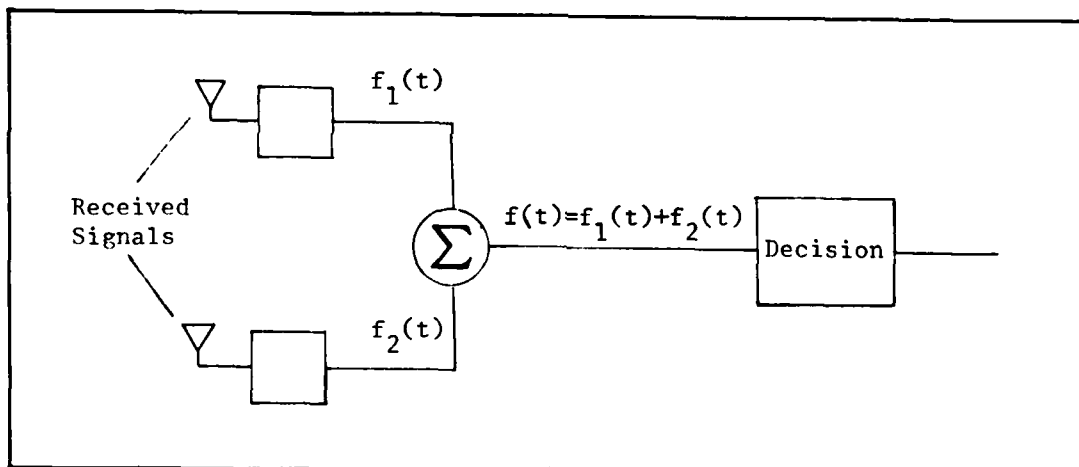


Figure 5.3  Equal Gain Diversity

## Analysis of Equal Gain Diversity

The combiner output SNR with ideal equal-gain combining is

$$\gamma_b = \sum_{K=1}^{L} \alpha_K{}^2 \cdot \frac{\mathcal{E}_b}{N_K} \qquad (5.24)$$

where

$\alpha_K$ = attenuation factor in Kth channel

$\mathcal{E}_b$ = energy per bit in the transmitted signal

$N_K$ = noise spectral power density in Kth channel

L = number of diversity channels

By assuming Rayleigh fading and equal noise in all channels, the p.d.f. of $\gamma_b$ for equal-gain diversity combining is developed by Schwartz et al., (20:456-7) as

$$p_D(\gamma_b) = \frac{2^{L-1} \, L^L \, (\gamma_b)^{L-1}}{(2L-1)! \, \prod\limits_{K=1}^{L} \overline{\gamma}_{CK}} \qquad (5.25)$$

where

$$\overline{\gamma}_{CK} = E\{\overline{\gamma}_{CK}\}$$

If we assume all diversity channels have equal mean SNR over the short-term fading, $\overline{\gamma}_{CK} = \overline{\gamma}_C$ then

$$p_D(\gamma_b) = \frac{2^{L-1} \, L^L \, (\gamma_b)^{L-1}}{(2L-1)! \, (\overline{\gamma}_C)^L} \qquad (5.26)$$

Now the probability of bit error can be calculated for the equal-gain diversity combining technique using DQPSK and 8-ary PSK.

For equal-gain diversity using DQPSK,

$$P_B(\text{DQPSK, equal-gain diversity}) = \int_0^\infty \frac{2^{L-1} \, L^L \, (\gamma_b)^{L-1}}{(2L-1)!(\overline{\gamma}_C)^L}$$

$$\cdot P_{B,\text{DQPSK}}(\gamma_b)d\gamma_b \qquad (5.27)$$

where

$$P_{B,DQPSK}(\gamma_b) = 2Q[(4\gamma_b\sin^2(\pi/8))^{0.5}]$$

For equal-gain diversity using 8-ary PSK,

$$P_B(8PSK, \text{ equal-gain diversity}) = \int_o^\infty \frac{2^{L-1} \; L^L \; (\gamma_b)^{L-1}}{(2L-1)!(\bar{\gamma}_c)^L}$$

$$\cdot P_{B,8PSK}(\gamma_b)d\gamma_b \qquad (5.28)$$

where

$$P_{B,8PSK}(\gamma_b) = \frac{2}{3} Q[(6\gamma_b)^{0.5}\sin(\pi/8)]$$

## Maximal Ratio

This diversity technique is similar to the equal gain method as the received channel signals, $f_j(t)$, are summed together to form the system output signal, $f(t)$; however, unlike the equal gain technique, maximal ratio requires that the gain of each channel is weighted by a factor proportional to its received signal strength (See Figure 5.4). Therefore, a strong received signal carries a larger weight and contributes more to the system output, $f(t)$, than a weak one. Each received channel signal is multiplied by the corresponding complex-valued (conjugate) channel gain $a_K$ exp ($j\phi K$) thus this type of combiner assumes that the channel attenuations and phase shifts are perfectly known (19:472).

Maximal ratio diversity is one of the most commonly used linear diversity combining techniques since it has been shown that it is the optimum combining method with respect to probability of error (3:1081 , 9:2-8). However, to obtain the proper weighting factors for each channel requires complex instrumentation. In a satellite communications downlink, a satellite beacon could provide the information needed
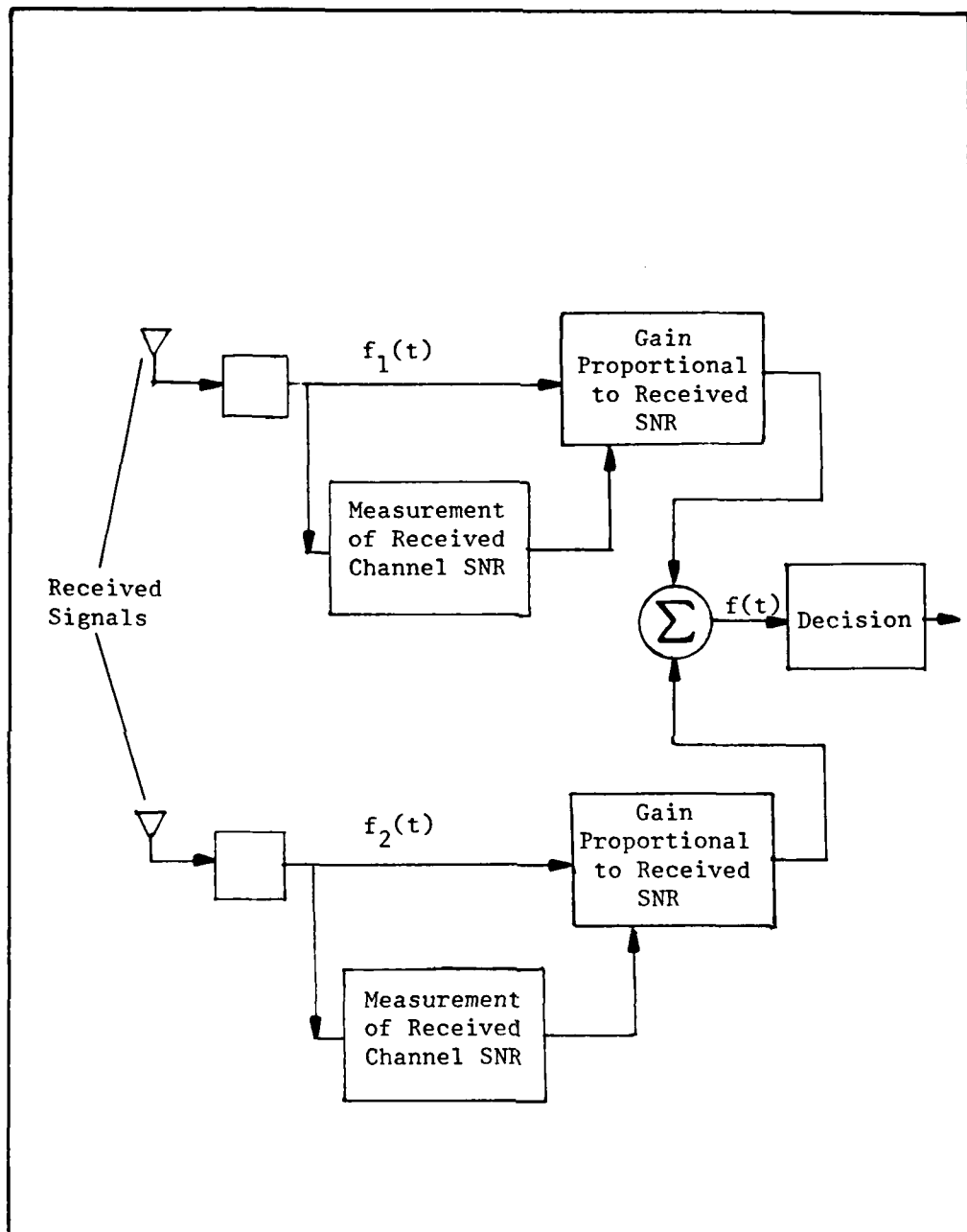
Figure 5.4  Maximal Ratio Diversity

to form the proper weighting factors. For this reason, some-
times equal gain or selection diversity is chosen since the
additional advantages of maximal ratio may not be large
enough to justify the additional cost of the equipment
needed to achieve the necessary maximal ratio combining.

Analysis of Maximal Diversity

The p.d.f. of the output SNR, $\gamma_b$, for a maximal ratio
combiner over short-term fading is developed by Schwartz
et al., (20:442-4). By taking the LaPlace transform of the
characteristic function of $\gamma_b$ and obtaining the inversion
of the transform, a complicated expression for $p_D(\gamma_b)$ is
obtained via contour integration. However, for the special
case when all average channel SNRs are equal during the
short term fading, this expression reduces to

$$p_D(\gamma_b) = \frac{1}{(L-1)!} \frac{(\gamma_b)^{L-1}}{(\bar{\gamma}_c)^L} \exp(-\gamma_b/\bar{\gamma}_c) \qquad (5.29)$$

Now the probability of bit error can be calculated for the
maximal-ratio diversity combining technique using DQPSK and
8-ary PSK.

For maximal ratio diversity using DQPSK,

$$P_B(\text{DQPSK, maximal ratio diversity}) = \int_o^\infty \frac{1}{(L-1)!} \frac{(\gamma_b)^{L-1}}{(\bar{\gamma}_c)^L} \exp(-\gamma_b/\bar{\gamma}_c)$$

$$\cdot P_B, \text{DQPSK}(\gamma_b) d\gamma_b \qquad (5.30)$$

where

$$P_{B,\text{DQPSK}}(\gamma_b) = 2Q[(4\gamma_b \sin^2(\pi/8)^{0.5}]$$

72

For maximal ratio diversity using 8-ary PSK,

$$P_B(\text{8PSK, maximal ratio diversity}) = \int_0^\infty \frac{1}{(L-1)!(\bar{\gamma}_c)^L} \frac{(\gamma_b)^{L-1}}{}$$

$$\cdot \exp(-\gamma_b/\bar{\gamma}_c)$$

$$\cdot P_B, \text{8PSK}(\gamma_b) d\gamma_b \quad (5.31)$$

where

$$P_B, \text{8PSK}(\gamma_b) = \frac{2}{3} Q[(6\gamma_b)^{0.5} \sin(\pi/8)]$$

An alternative method to calculate the probability of bit error for maximal ratio diversity systems is developed by Proakis in Ref 19. Proakis (19:490) develops a general result for the probability of a symbol error in M-ary PSK systems using maximal ratio diversity

$$P_M = \frac{(-1)^{L-1}(1-u^2)^L}{\pi (L-1)!} \left(\frac{\partial^{L-1}}{\partial_b^{L-1}} \left\{ \frac{1}{b-u^2} \left[ \frac{\pi}{M} (M-1) \right. \right.$$

$$\left. \left. - \frac{u \sin(\pi/M)}{[b-u^2\cos^2(\pi/M)]^{0.5}} \cot^{-1}\left(\frac{-u\cos \cos(\pi/M)}{[b-u^2\cos^2(\pi/M)]^{0.5}}\right) \right] \right\} \right)$$

$$(5.32)$$

where

$$\mu = [\bar{\gamma}_c/(1 + \bar{\gamma}_c)]^{0.5} \text{ for coherent PSK}$$

$$\mu = \bar{\gamma}_c/(1 + \bar{\gamma}_c) \text{ for DPSK}$$

$$\bar{\gamma}_c = \text{average SNR per channel} = \frac{E\{\alpha_K^2\}\mathcal{E}}{N_o}$$

$\mathcal{E}$ = energy in transmitted signal

$$\gamma_b = \text{average bit SNR} = \frac{L \, \bar{\gamma}_c}{K}$$

$$K = \log_2 M$$

The bit error rate for DQPSK with maximal ratio diversity is derived by Proakis assuming a Gray code (See Figure 5.5). The probability of bit error is calculated by

$$P_B(\text{DQPSK, maximal ratio diversity}) = \sum_{K=1}^{2} (K \text{ errors}) \cdot (P_{eK}) \quad (5.33)$$
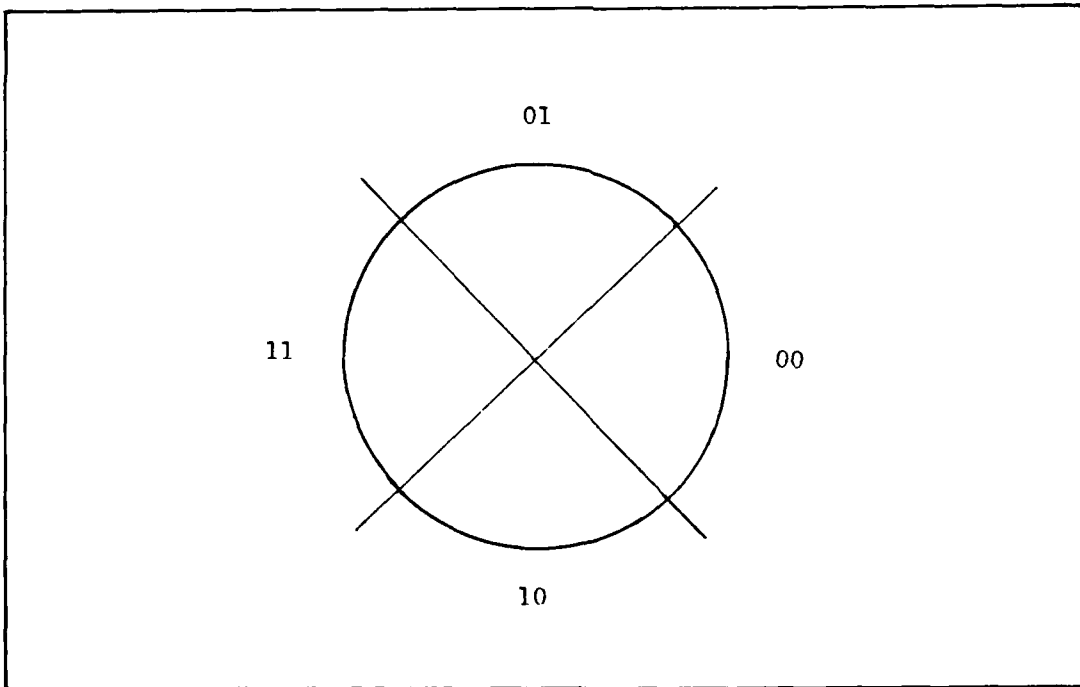
where

$P_{eK}$ = probability of error for K bit errors



Figure 5.5   4-ary Gray Code

The resulting expression for probability of bit error for DQPSK with maximal ratio diversity is

$$P_B(\text{DQPSK, maximal ratio diversity}) = 0.5 \left[1 - \frac{\mu}{(2-\mu^2)^{0.5}} \sum_{K=0}^{L-1} \right.$$

$$\left. \binom{2K}{K} \left(\frac{1-\mu^2}{4-2\mu^2}\right)^K \right] \qquad (5.34)$$

where

$$\mu = \left[\bar{\gamma}_c / (1 + \bar{\gamma}_c)\right]^{0.5}$$

Using the same method used by Proakis for obtaining Eq (5.34), the probability of bit error for an 8-ary PSK signal with maximal ratio diversity can be generated by evaluating Eq (5.5) where

$\int_{\theta_1}^{\theta_2} P(\theta)d\theta$ is defined by Proakis [Eq (7A.14), Ref 19:532)] as

$$\int_{\theta_1}^{\theta_2} p(\theta)d\theta = \frac{(-1)^{L-1}(1-\mu^2)^L}{2\pi(L-1)!} \frac{\partial^{L-1}}{\partial b^{L-1}} \left(\frac{1}{b-\mu^2} \left\{ \frac{\mu(1-[(b/\mu^2)-1]x^2)^{0.5}}{b^{0.5}} \right. \right.$$

$$\left. \left. \cdot \cot^{-1}X - \cot^{-1}\left(\frac{(Xb^{0.5}/\mu)}{1-[b(\mu^2)-1]x^2)^{0.5}}\right) \right\} \right) \left. \begin{matrix} X_2 \\ X_1 \end{matrix} \right|_{b=1} \qquad (5.35)$$

where

$$X_i = \frac{-\mu \cos\theta i}{(b-\mu^2 \cos\theta i)^{0.5}} , \quad i = 1,2$$

$$\mu = \left[\bar{\gamma}_c / (1 + \bar{\gamma}_c)\right]^{0.5}$$

75

# VI.  Computer Program Development

Having developed the equations needed to calculate the probability of bit error for the different combinations of diversity techniques and digital signaling schemes, it was necessary to develop a computer program to obtain the desired calculations.  In order to reduce run time, I wrote a separate program in Fortran 77 for each diversity technique/digital signaling scheme combination.  Including the case of no diversity (i.e., the probability of bit error for DQPSK and 8-ary PSK with no diversity), there are seven programs used to calculate the probability of bit error calculations.

## Choice of Range of Variables

The computer results were to be plotted as the probability of bit error versus the signal-to-noise ratio (SNR) per bit.  Therefore, a range for the SNR per bit needed to be chosen.  Considering the range (5-40 dB) chosen in similar graphs presented in Ref 19, the range for bit SNR was chosen as 10-40 in decibels.  A determination was also made on the maximum number of diversity channels for probability of error calculations.  Since the use of more than two diversity channels in a satellite communications diversity system is rare, I limited the probability of bit error calculations for the six different diversity/signaling scheme combinations to 2, 3, and 4 diversity channels.  Therefore, the final results for the six combinations can be compared over the bit SNR

76

range of 10-40 decibels for 2, 3, and 4 diversity terminals.
Likewise, these results can be compared to the case of no
diversity to determine the benefits of the diversity system.

## Equations Used to Calculate Probability of Bit Error

The equations needed to calculate the probability of bit
error for all of the diversity/signaling scheme combinations
were developed in Section V. The equations from Section V
used in the computer programs are listed below:

| | |
|---|---|
| DQPSK w/no diversity | Eq (5.10) |
| 8-ary PSK w/no diversity | Eq (5.11) |
| Selection diversity w/DQPSK | Eq (5.21) |
| Selection diversity w/8-ary PSK | Eq (5.22) |
| Equal Gain diversity w/DQPSK | Eq (5.27) |
| Equal Gain diversity w/8-ary PSK | Eq (5.28) |
| Maximal Ratio diversity w/DQPSK | Eq (5.30) |
| Maximal Ratio diversity w/8-ary PSK | Eq (5.31) |

All of the equations listed above require the solution
to an indefinite integral. For the maximal ratio case, an
alternative method for obtaining the probability of bit error
for DQPSK and 8-ary PSK is stated in Eqs (5.34) and (5.35),
respectively. The difficulties in getting the required par-
tial derivatives for this method resulted in the deletion of
this method.

## Solving the Indefinite Integral

The choice of Fortran 77 as the programming language for the programs for calculating the probability of bit error was primarily due to the mathematical and statistical library available in Fortran. In order to solve the indefinite integrals needed to find the probabilities of bit error, I used the DCADRE subroutine from the IMSL software library. The DCADRE subroutine performs a numerical integration of a function using cautious adaptive Romberg extrapolation.

The indefinite integrals in the equations for evaluating the probability of error were approximated by using a piecewise summation of the integration. The integral from zero to infinity is approximated by the piecewise integral from $1 \times 10^{-15}$ to the point where the area of this last subinterval is less than 0.000001 of the summation of its area plus all previously calculated subinterval areas. This approximation works satisfactorily since the product of the p.d.f. of the diversity technique and the conditional probability of bit error given the bit SNR is always positive and the limit of this product approaches zero as bit SNR approaches infinity.

The DCADRE subroutine requires that the integrand of the integral be supplied by the user in the form of a function. For each diversity/signaling scheme combination, the product of the p.d.f. and conditional probability was expressed as a Fortran function so the DCADRE function could calculate the subinterval area. In order to calculate the conditional

78

probability of a bit error for the digital signaling scheme within this function, another subroutine from the IMSL software library was needed.

The IMSL subroutine MERFD=DERF was used to evaluate the mathematical error function of a double precision argument. This subroutine computes the value of the integral

$$\text{derf}(Y) = (2/\pi) \int_{o}^{Y} \exp(-t^2) \, dt \qquad (6.1)$$

where

Y = argument of the mathematical error function

By performing the following conversion, the Q function defined by Eq (2.25.a) can be expressed as a function of the IMSL subroutine MERFD=DERF.

$$Q(x) = 1 - [(\text{derf}(x/2^{0.5}) + 1)/2] \qquad (6.2)$$

Therefore, the conditional probabilities in the integrand of the indefinite integral can be expressed in the Q function form within the Fortran function needed by the DCADRE subroutine.

## Validation of Computer Results

The computer results for the DQPSK with no diversity and DQPSK with maximal ratio diversity cases were compared to the results presented by Proakis in Ref G, Chapter 7. For each case, the results were similar, although my probability of bit error curves are slightly shifted to the right of Proakis' curves (i.e., for both cases my results show

79

slightly higher probability of bit error rates than Proakis).
The most likely cause of this difference is the approxima-
tion used for DQPSK [Eq (5.2)]. However, the accuracy of
the computer results is well within the range to validate
the approach used to compute the probability of bit error.
Since all seven programs were written using the same approach,
it is assumed that all the computer results are reasonably
accurate and in particular, the results are accurate for
assessing the relative performance of the diversity schemes.

## Computer Program for Calculation of Rain Attenuation

In addition to the programs for calculating the proba-
bility of bit error, a program was developed to calculate the
attenuation per unit distance, A, based on the approximate
relation between A and the rain rate R, where $A = aR^b$, des-
cribed in Eq (3.2). The values for the coefficients a and
b were obtained for three different rain temperatures,
-10°C, 0°C, and 20°C. These values were obtained from Tables
3.2, 3.3, and 3.4 using a downlink frequency of 20 GHz and a
Marshall-Palmer (MP) raindrop size distribution. The rain
attenuation per unit distance will be calculated as decibels/
kilometers and the rain rate will vary from 5 mm/hr to
100 mm/hr.

# VII. <u>Results</u>

The data obtained from the computer programs described
in Section VI are discussed in the following pages. By exam-
ining the data, an evaluation of the different diversity/
signaling scheme combinations can be obtained to determine
the benefits of using a diversity network. Comparisons be-
tween the different diversity techniques will illustrate
which technique yields the maximum benefits.

## Analysis of Diversity Benefits

By using the HP-7229 plotter, the results of the com-
puter programs were plotted to obtain the graphs of the prob-
ability of bit error versus the SNR per bit for each diver-
sity/signaling scheme combination. These graphs are depicted
in the following figures:

|  |  |
|---|---|
| DQPSK and 8-ary PSK w/No Diversity | Figure 7.1 |
| Selection Diversity w/DQPSK | Figure 7.2 |
| Selection Diversity w/8-ary PSK | Figure 7.3 |
| Equal Gain Diversity w/DQPSK | Figure 7.4 |
| Equal Gain Diversity w/8-ary PSK | Figure 7.5 |
| Maximum Ratio Diversity w/DQPSK | Figure 7.6 |
| Maximum Ratio Diversity w/8-ary PSK | Figure 7.7 |

By looking at Figures 7.1 - 7.7, it is obvious that the use of a diversity technique greatly reduces the probability of bit error in a Rayleigh fading channel. It is also apparent that regardless of which diversity/signaling scheme is used, the probability of bit error reduces as the order of diversity of channels increases. A more indepth look at the diversity benefits are depicted in Tables 7.1 - 7.4.

As displayed in Tables 7.1 and 7.2, the benefits of diversity techniques are significant. Table 7.1 shows the benefits of the selected diversity techniques with DQPSK compared to DQPSK without diversity and Table 7.2 shows the benefits of the selected diversity techniques with 8-ary PSK compared to 8-ary PSK without diversity. For each case, as the average SNR per bit increases, the benefits of the diversity network increases. For example, given a received average bit SNR of 40 dB for a DQPSK (8-ary PSK) w/no diversity system, the minimum diversity gain is 18.25 dB (20.0 dB) when using selection diversity with two channels and the maximum diversity gain is 26 dB (27.25 dB) when using maximal ratio diversity with four channels. Likewise, for a received average bit SNR of 60 dB, the diversity gain for selection diversity with two channels is 28.25 dB (30.0 dB) and the diversity gain for maximal ratio diversity with four channels is 40.5 dB (41.75 dB).

The data displayed in Tables 7.3 and 7.4 allows for a comparison of all six diversity/signaling scheme combinations.

Two significant conclusions can be made from this data:

1. The maximal ratio diversity technique provides the most diversity gain, followed by equal gain diversity and lastly selection diversity.

2. The diversity/signaling scheme combinations with 8-ary PSK outperform the same combinations with DQPSK. (The latter conclusion may partially result from the approximation used for DQPSK). Based on these results, the optimum diversity/signaling scheme combination of the six is the maximal ratio diversity technique with 8-ary PSK.

Other important considerations regarding the selection of a diversity technique for a satellite communications system is the cost of implementing the diversity technique. As denoted in Section V, maximal ratio diversity requires the use of a satellite beacon to properly weigh the received channel signals. Although maximal ratio diversity provides the best diversity gain, it is also the most costly to implement due to the additional equipment needed to obtain the satellite beacon information and translate it into correct weighing factors. Thus, there is a direct trade-off between cost and performance in the selection of the diversity technique and the number of earth stations used in the satellite communications diversity system.

Analysis of Rain Attenuation for Downlink

The rain attenuation for a satellite communications downlink can be estimated from the data presented in Figures 7.8

83

and 7.9. In Figure 7.8, the rain attenuation per unit distance (dB/km) can be approximated by knowing the rain rate for rain temperatures of 20°C, 0°C, and -10°C. Given the rain rate and the angle of elevation of the receiving satellite terminal, the effective path length (in km) can be estimated using Figure 7.9.

Therefore, the approximate rain attenuation (in dB) can be obtained by multiplying the effective path length determined from Figure 7.9 and the rain attenuation per unit distance indicated from Figure 7.8. By knowing the approximate rain attenuation, its effect of the probability of a bit error can be determined from Figures 7.1 - 7.7. By subtracting the rain attenuation from a given received bit SNR for a diversity/signaling scheme for a satellite communications downlink without rainfall effects, the corresponding probability of bit error can be obtained. The increase in the probability of bit error is the result of the rain attenuation. Therefore, the effects of rain attenuation for different rain rates and different elevation angles on the six different diversity/signaling scheme combinations can be estimated using Figures 7.1 - 7.9.

For example, assume a maximal ratio diversity system with two channels using 8-ary PSK for a downlink earth station with an angle of elevation of 40° operating during clear weather conditions. For an average received SNR per bit of 20 dB, the probability of bit error obtained from Figure 7.7 is $2.807 \times 10^{-5}$. Now assume a rain rate of 25 mm/hr and a

rain temperature of 20°C.  From Figure 7.8, the rain attenuation is ~2.6 dB/km and from the effective path length of ~4.4 km is obtained from Figure 7.9.  Thus, the rain attenuation is ~11.44 dB and the effective average received SNR per bit for the diversity system is now ~9.5 dB with a probability of bit error of 2.786 x $10^{-3}$.  Obviously, the detrimental effect of rain attenuation on the performance of satellite communications systems is very significant.
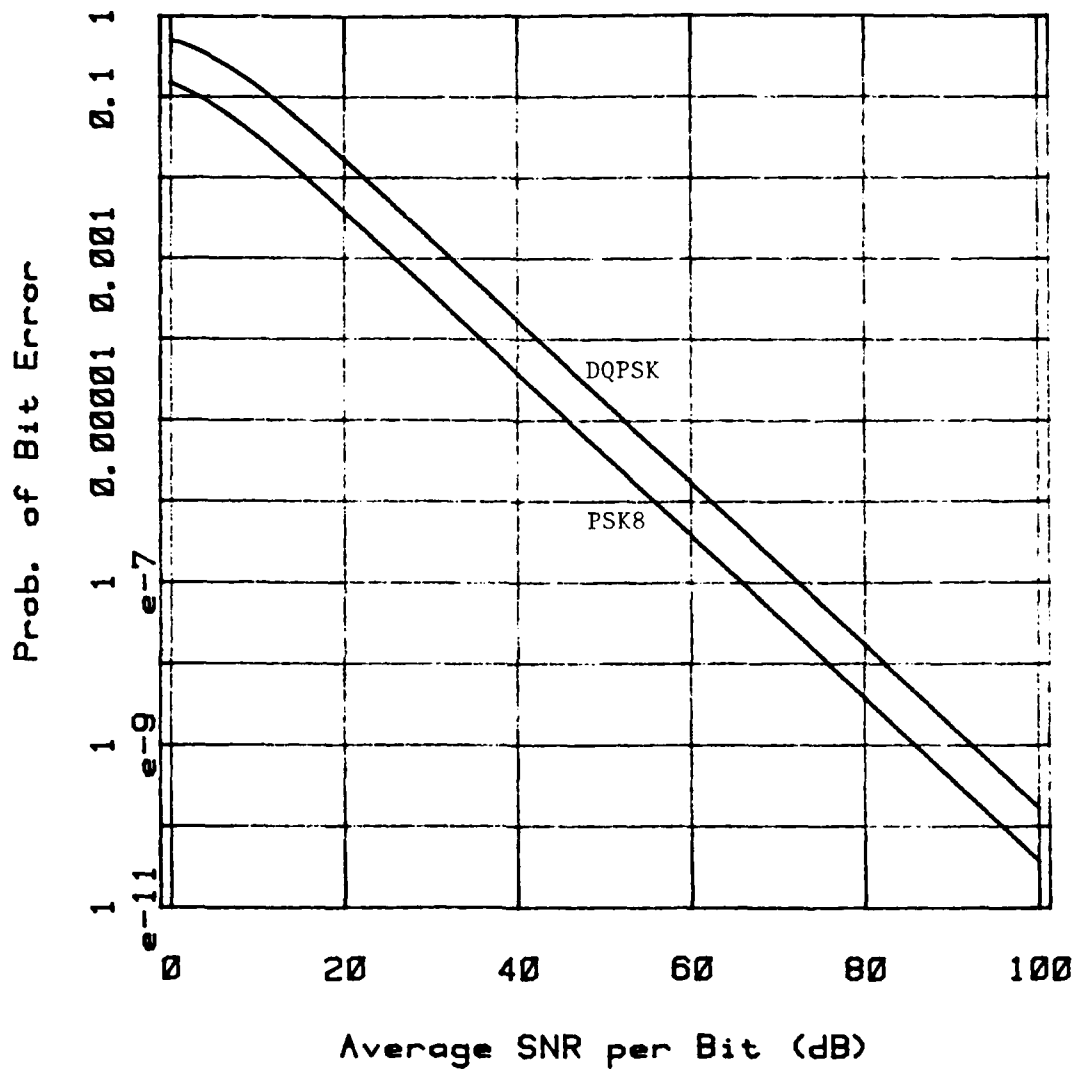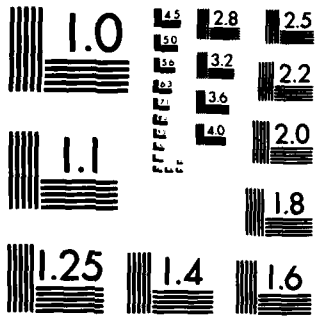
Figure 7.1  DQPSK and 8-ary PSK w/No Diversity

86

END

FILMED

DTIC

MICROCOPY RESOLUTION TEST CHART
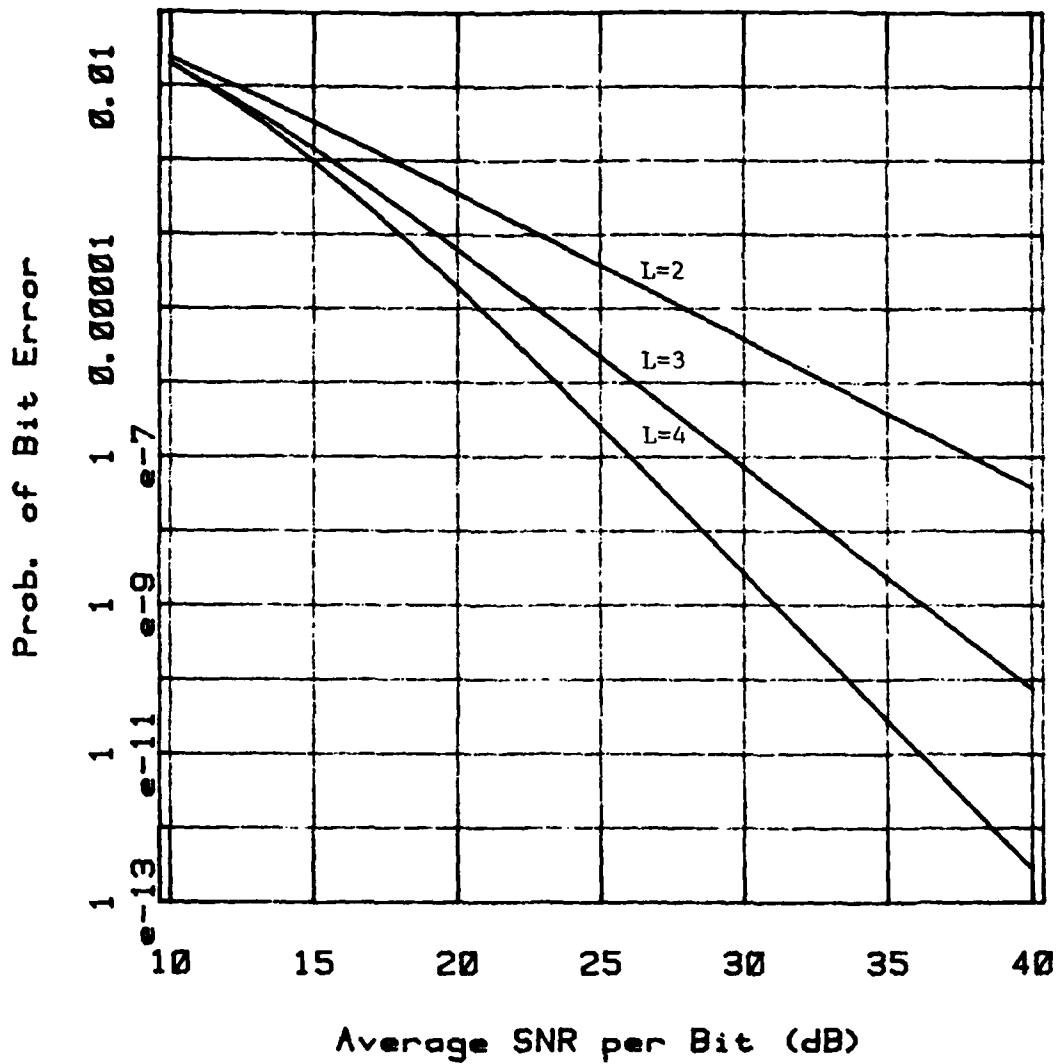
NATIONAL BUREAU OF STANDARDS-1963-A

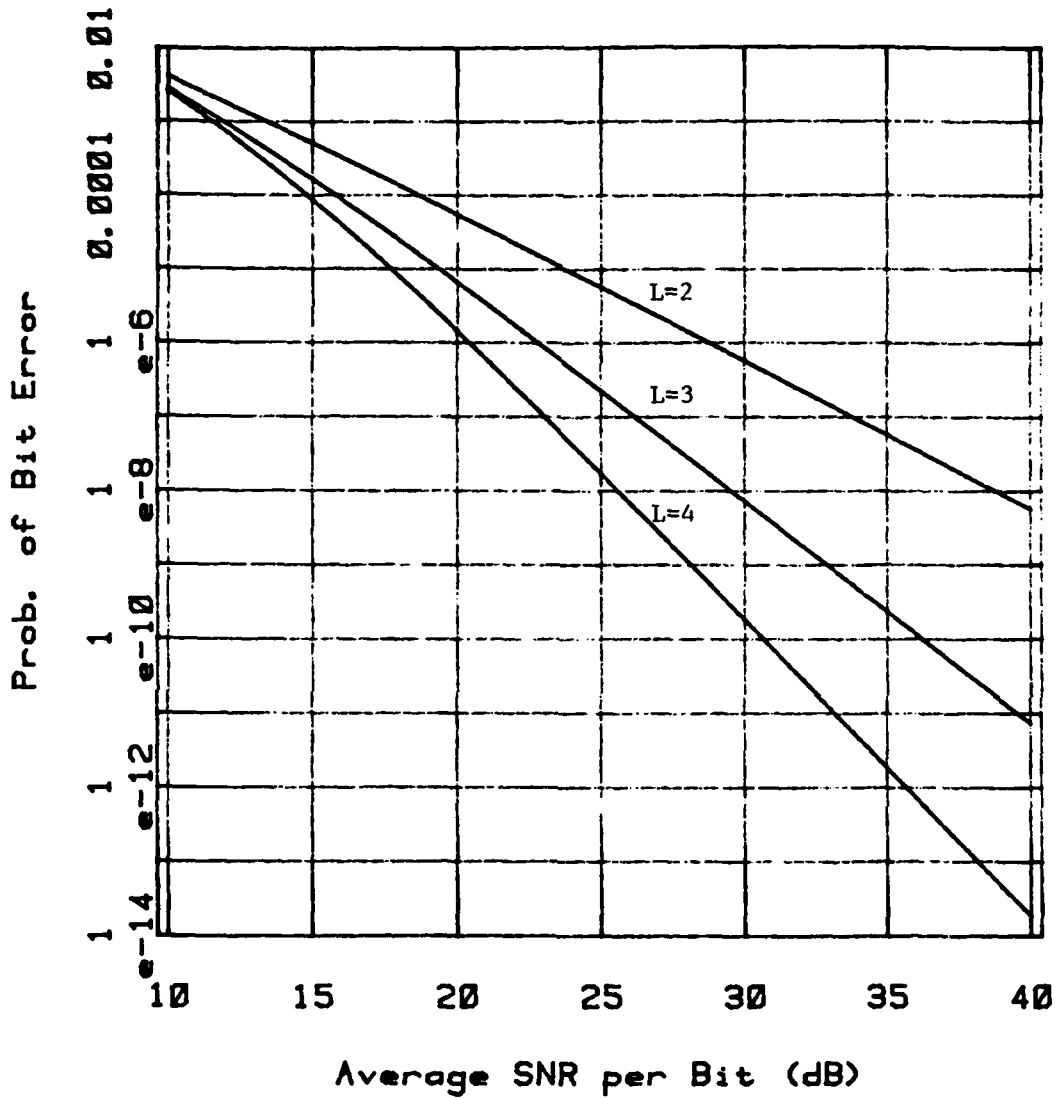Figure 7.2   Selection Diversity w/DQPSK

87

Figure 7.3  Selection Diversity w/8-ary PSK
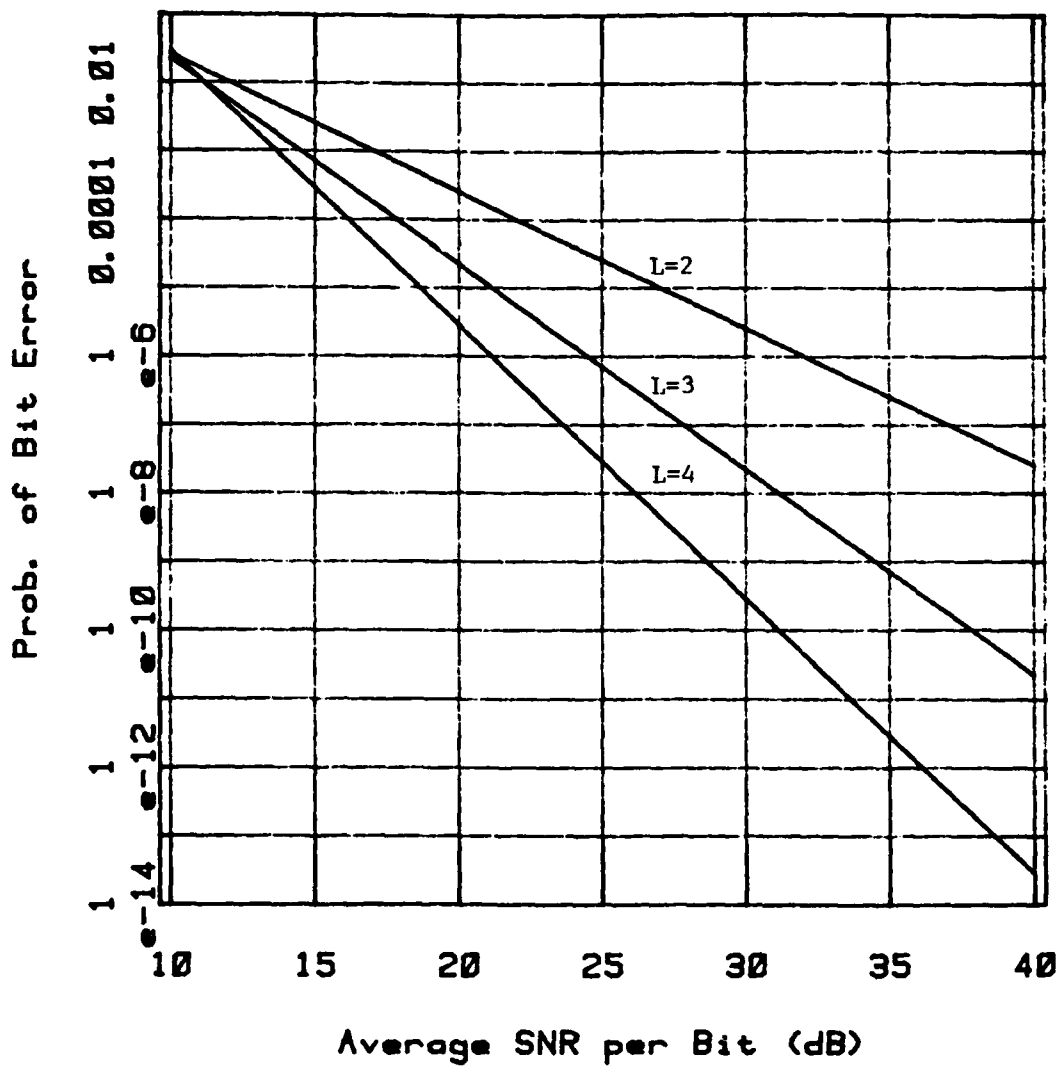
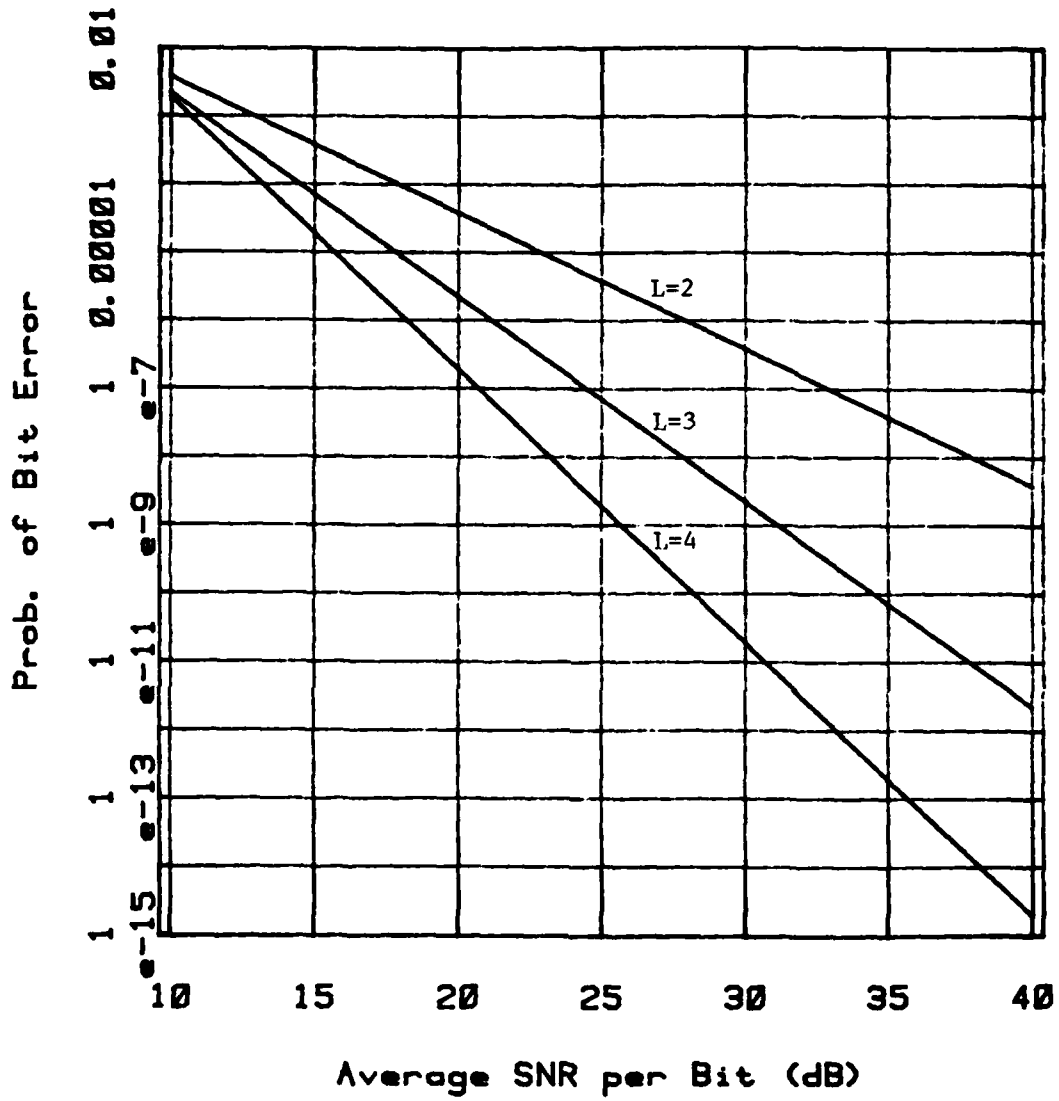Figure 7.4   Equal Gain Diversity w/DQPSK

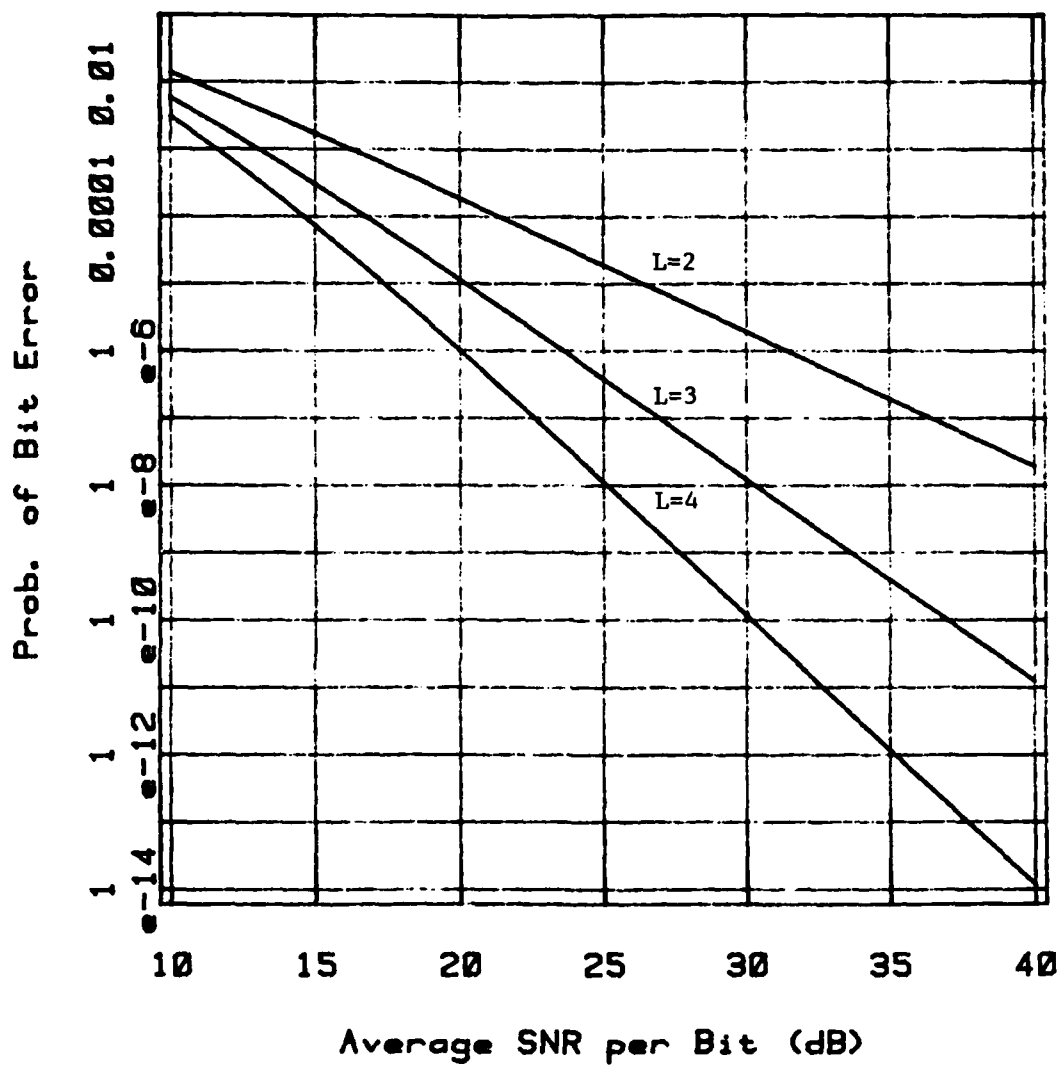Figure 7.5   Equal Gain Diversity w/8-ary PSK

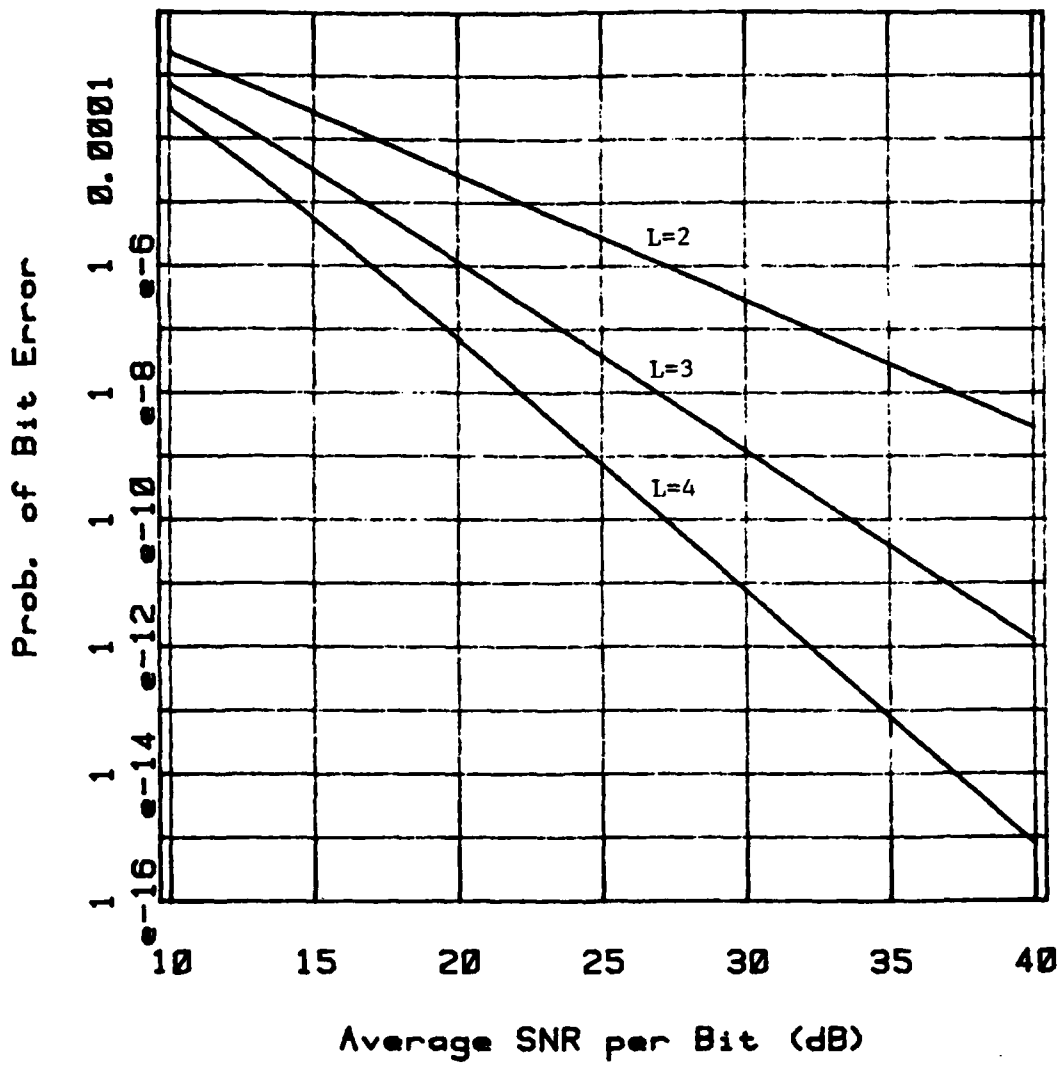Figure 7.6   Maximal Ratio Diversity w/DQPSK

Figure 7.7   Maximal Ratio Diversity w/8-ary PSK

92

TABLE 7.1

Comparison of Selected Diversity Techniques w/DQPSK to DQPSK w/No Diversity

| | | Probability of Bit Error | | | | |
|---|---|---|---|---|---|---|
| | | $1.660 \times 10^{-2}$ | $1.702 \times 10^{-4}$ | $1.703 \times 10^{-6}$ | $1.703 \times 10^{-8}$ | $1.703 \times 10^{-10}$ |
| | DQPSK w/no Diversity | 20.0dB | 40.0dB | 60.0dB | 80.0dB | 100.0dB |
| Selection Diversity | 2 channels | 11.0 | 21.75 | 31.75 | 41.75 | 51.75 |
| | 3 channels | 10.5 | 18.5 | 25.25 | 32.0 | 39.5 |
| | 4 channels | 10.5 | 17.25 | 22.75 | 28.0 | 33.25 |
| Equal Gain Diversity | 2 channels | 11.5 | 20.75 | 31.0 | 41.0 | 51.0 |
| | 3 channels | 10.75 | 17.0 | 23.75 | 30.25 | 37.75 |
| | 4 channels | 10.75 | 15.5 | 20.5 | 25.5 | 30.75 |
| Maximal Ratio Diversity | 2 channels | 9.5 | 20.25 | 30.25 | 40.25 | 50.25 |
| | 3 channels | 8.0 | 16.0 | 22.75 | 29.5 | 36.5 |
| | 4 channels | 7.25 | 14.0 | 19.5 | 24.5 | 29.75 |

Average $\frac{E_b}{N_o}$ Needed to Achieve Prob. of Bit Error Performance

TABLE 7.2

Comparison of Selected Diversity Techniques w/8-ary PSK to 8-ary PSK w/No Diversity

Probability of Bit Error

| 8-ary PSK w/ no Diversity | | $3.720 \times 10^{-3}$ | $3.783 \times 10^{-5}$ | $3.784 \times 10^{-7}$ | $3.784 \times 10^{-9}$ | $3.784 \times 10^{-11}$ |
|---|---|---|---|---|---|---|
| | | 20.0dB | 40.0dB | 60.0dB | 80.0dB | 100.0dB |
| Selection Diversity | 2 channels | 10.25 | 21.0 | 31.0 | 40.75 | 51.25 |
| | 3 channels | 9.5 | 17.25 | 24.25 | 31.0 | 37.75 |
| | 4 channels | 9.25 | 16.0 | 21.5 | 26.75 | 31.75 |
| Equal Gain Diversity | 2 channels | 10.0 | 20.0 | 30.0 | 40.0 | 50.0 |
| | 3 channels | 9.25 | 16.0 | 22.5 | 29.25 | 36.0 |
| | 4 channels | 9.25 | 14.25 | 19.25 | 24.25 | 29.25 |
| Maximal Ratio Diversity | 2 channels | 8.75 | 19.25 | 29.5 | 39.75 | 49.25 |
| | 3 channels | 7.0 | 14.75 | 21.75 | 28.5 | 35.5 |
| | 4 channels | 6.0 | 12.75 | 18.25 | 23.25 | 28.5 |

Average $\frac{E_b}{N_o}$ Needed to Achieve Prob. of Bit Error Performance

94

## TABLE 7.3

Comparison of Selected Diversity Techniques w/DQPSK
with Respect to Probability of Bit Error

Probability of Bit Error

| | | $10^{-3}$ | $10^{-4}$ | $10^{-6}$ | $10^{-8}$ | $10^{-10}$ | $10^{-12}$ |
|---|---|---|---|---|---|---|---|
| Selection Diversity | 2 channels | 17.75dB | 23.0dB | 33.0dB | 43.0dB | 53.0dB | 63.0dB |
| | 3 channels | 15.5 | 19.25 | 26.25 | 33.0 | 39.5 | 46.25 |
| | 4 channels | 15.0 | 18.0 | 23.5 | 28.5 | 33.5 | 38.5 |
| Equal Gain Diversity | 2 channels | 17.0 | 22.0 | 32.0 | 42.0 | 52.0 | 62.0 |
| | 3 channels | 14.5 | 17.75 | 24.5 | 31.25 | 37.75 | 44.5 |
| | 4 channels | 13.75 | 16.25 | 21.25 | 26.25 | 31.25 | 36.25 |
| Maximal Ratio Diversity | 2 channels | 16.25 | 21.25 | 31.5 | 41.5 | 51.5 | 61.5 |
| | 3 channels | 13.0 | 16.75 | 23.5 | 30.25 | 37.0 | 43.75 |
| | 4 channels | 25.25 | 14.5 | 20.0 | 25.0 | 30.25 | 35.25 |

Average $\frac{E_b}{N_o}$ Needed to Achieve Prob. of Bit Error Performance

TABLE 7.4

Comparison of Selected Diversity Techniques w/8-ary PSK
with Respect to Probability of Bit Error

Probability of Bit Error

| | | $10^{-3}$ | $10^{-4}$ | $10^{-6}$ | $10^{-8}$ | $10^{-10}$ | $10^{-12}$ |
|---|---|---|---|---|---|---|---|
| Selection Diversity | 2 channels | 13.5dB | 18.75dB | 28.75dB | 38.75dB | 48.75dB | 58.75dB |
| | 3 channels | 12.0 | 15.75 | 22.75 | 29.5 | 36.25 | 43.0 |
| | 4 channels | 11.5 | 14.75 | 20.5 | 25.5 | 30.75 | 35.75 |
| Equal Gain Diversity | 2 channels | 13.0 | 18.0 | 28.0 | 37.75 | 48.0 | 58.0 |
| | 3 channels | 11.25 | 14.5 | 21.25 | 27.75 | 34.5 | 41.25 |
| | 4 channels | 10.75 | 13.25 | 18.25 | 23.25 | 28.25 | 33.25 |
| Maximal Ratio Diversity | 2 channels | 12.0 | 17.0 | 27.25 | 37.25 | 47.25 | 57.25 |
| | 3 channels | 9.5 | 13.25 | 20.25 | 27.0 | 33.5 | 40.25 |
| | 4 channels | 8.25 | 11.5 | 17.0 | 22.5 | 27.25 | 32.50 |

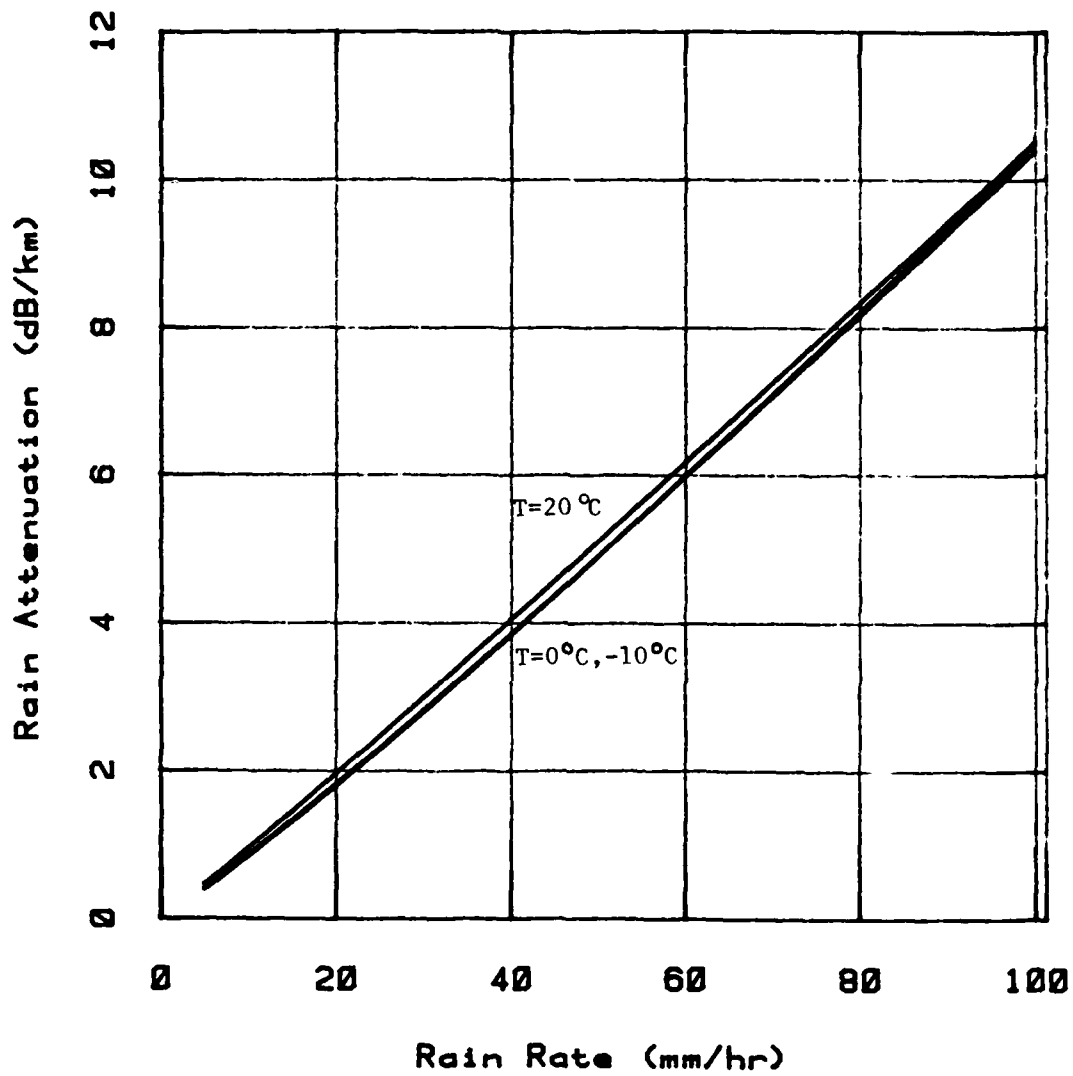Average $\frac{E_b}{N_o}$ Needed to Achieve Prob. of Bit Error Performance

96

Figure 7.8   Rain Attenuation Using A = aR$^b$ Relationship
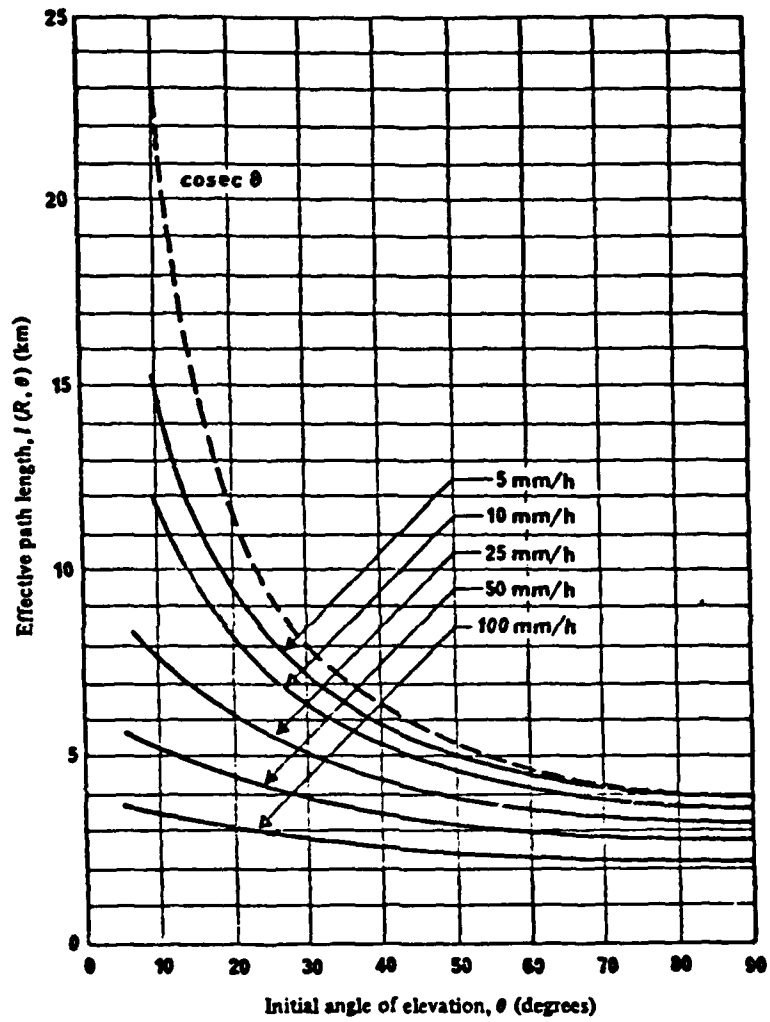
Figure 7.9   Effective Path Length for Rain Rates

Source: (5:224)

## VIII. Conclusions and Recommendations

### Conclusions

On the basis of the computer results of the performance of diversity techniques in the downlink reception equipment for satellite communications systems, the following conclusions are made:

1.  The best link parameter to use in the process of determining the received signal in a diversity system is the received channel SNR or some variation of it such as average SNR per bit.

2.  Of the three diversity techniques evaluated, maximal ratio diversity provided the optimum diversity benefits followed by equal gain diversity and lastly selection diversity. However, all three diversity methods provide significant improvement of bit error performance when compared to a similar system without diversity. These diversity combining techniques can be used to combat rain attenuation or to improve the overall reception characteristics.

3.  Regardless of which diversity technique is used, as the number of channels used increases, tne bit error performance improves.

4.  Maximal ratio diversity requires the use of a satellite beacon while equal gain and selection diversity do not. Thus, additional equipment is needed in a maximal ratio diversity reception system thereby increasing the cost.

5. The diversity/signaling combinations using 8-ary PSK provided a slightly better bit error performance than its counterpart using DQPSK.

6. The effects of rain attenuation on a diversity downlink reception system can be estimated by applying the results of this study.

## Recommendations

Based on the observations made during this investigation, the following recommendations are proposed for further study:

1. This study assumed perfect synchronization; the effects of the loss of synchronization on bit error performance should be investigated.

2. The results of this study could be applied to rainfall statistics to obtain theoretical long-range uptime and downtime statistics for downlink diversity reception systems located in various geographical locations.

## Bibliography

1. Allnutt, J.E. "Nature of Space Diversity in Microwave Communications via Geostationary Satellites: A Review," Proc. IEE, 5: 369-376 (May 1978).

2. Bhargava, Vijay K. and others. Digital Communications By Satellite. New York: Wiley-Interscience Publication, 1981.

3. Brennan, D.G. "Linear Diversity Combining Techniques," Proceedings of the IRE, 47: 1075-1102 (June 1959).

4. Castor, Kenneth G. Lecture materials distributed in EE 6.70, Principles of Digital Communications. School of Engineering, Air Force Institute of Technology (AU), Wright-Patterson AFB OH, April 1984.

5. CCIR, Recommendations and Reports of the CCIR, 1978, "Propagations Data Required for Telecommunication Systems," Report 564-1, Geneva, 1978, Vol V: 219-239.

6. Crane, R.K. "Prediction of the Effects of Rain on Satellite Communications Systems," Proceedings of the IEEE, 65: 456-474 (March 1977).

7. -----. "Propagation Phenomena Affecting Satellite Communication Systems Operating in the Centimeter and Millimeter Wavelength Bands," Proceedings of the IEEE, 59: 173-188 (February 1971).

8. Defense Communications Agency. Rainfall Attenuation at 30/20 GHz. Contract No. DCA100-76-C-0089, Task Order No. 0508, April 1981.

9. Defense Communications Agency. Analysis of Diversity For 30/20 GHz Satellite Communications. Contract No. DCA100-76-C-0089, Task Order No. 0307, August 1979.

10. Engelbrecht, R. S., "The Effect of Rain on Satellite Communications Above 10 GHz." RCA Review, 40: 191-229 (June 1979).

11. Gagliardi, Robert M. Satellite Communications. Belmont CA: Lifetime Learning Publications, 1984.

12. Hodge, D.B. "An Improved Model for Diversity Gain on Earth-Space Propagation Paths," Radio Science, 17: 1393-1399 (November-December 1982).

13. ------. "An Empirical Relationship for Path Diversity Gain," <u>IEEE Transactions on Attennas and Propagations</u>, AP-24, <u>No. 2</u>: 250-251 (1976).

14. Hogg, D.C. and Chu, Ta-Shing. "The Role of Rain in Satellite Communications," <u>Proceedings of the IEEE</u>, <u>63</u>: 1308-1331 (September 1975).

15. Lin, S.H. "Statistical Behavior of Rain Attenuation," <u>Bell System Technical Journal</u>, <u>52</u>: 557-581 (April 1973).

16. Martin, James. <u>Communications Satellite Systems</u>. Englewood Cliffs NJ: Prentice-Hall, Inc., 1978.

17. Mie, G. <u>Annalen der Physik (4)</u>, <u>Vol. 25</u>: 377 (1908).

18. Olsen, R.L. and others. "The $aR^b$ Relation in the Calculation of Rain Attenuation," <u>IEEE Transactions on Antennas and Propagations</u>, AP-26, <u>No. 2</u>: 318-329 (March 1978).

19. Proakis, John G. <u>Digital Communications</u>. New York: McGraw-Hill Co., 1983.

20. Schwartz, M. and others. <u>Communications Systems and Techniques</u>. New York: McGraw-Hill Co., 1966.

21. Shanmugam, K.S. <u>Digital and Analog Communications Systems</u>. New York: Wiley & Sons, Inc., 1979.

22. Spilker, J.J. <u>Digital Communications By Satellite</u>. Englewood Cliffs NJ: Prentice-Hall, Inc., 1977.

23. Ziemer, R.E. and Tranter W.H. <u>Principles of Communications Systems, Modulation, and Noise</u>. Boston: Houghton Mifflin Co., 1976.

VITA

Captain Steven L. Skipper was born 26 April 1957 in Fairbanks, Alaska. He graduated from high school in Tampa, Florida in 1975 and attended the University of Florida from which he received the degree of Bachelor of Science in Electrical Engineering in March 1980. Upon graduation, he received a commission in the USAF through the ROTC program and entered the Air Force on active duty in April 1980. He completed the Communications-Electronics Officer School at Keesler, AFB Mississippi in October 1980. He then served as a Communications-Electronics Engineer and Chief of Maintenance in the 1928th Communications Group, MacDill AFB, Florida, until entering the School of Engineering, Air Force Institute of Technology, in May 1982.

Permanent Address: Route 1, Box 1456

Plant City, Florida 33566

SECURITY CLASSIFICATION OF THIS PAGE

## REPORT DOCUMENTATION PAGE

| REPORT SECURITY CLASSIFICATION<br>UNCLASSIFIED | | 1b. RESTRICTIVE MARKINGS |
|---|---|---|
| 2a. SECURITY CLASSIFICATION AUTHORITY | | 3. DISTRIBUTION/AVAILABILITY OF REPORT |
| 2b. DECLASSIFICATION/DOWNGRADING SCHEDULE | | Approved for public release; distribution unlimited. |
| 4. PERFORMING ORGANIZATION REPORT NUMBER(S)<br>AFIT/GE/ENG/84D-61 | | 5. MONITORING ORGANIZATION REPORT NUMBER(S) |

| 6a. NAME OF PERFORMING ORGANIZATION<br>School of Engineering | 6b. OFFICE SYMBOL<br>(If applicable)<br>AFIT/ENG | 7a. NAME OF MONITORING ORGANIZATION |
|---|---|---|
| 6c. ADDRESS (City, State and ZIP Code)<br>Air Force Institute of Technology<br>Wright-Patterson AFB, Ohio 45433 | | 7b. ADDRESS (City, State and ZIP Code) |

| 8a. NAME OF FUNDING/SPONSORING ORGANIZATION Defense Communications Eng. Ctr. | 8b. OFFICE SYMBOL<br>(If applicable)<br>DCEC/R420 | 9. PROCUREMENT INSTRUMENT IDENTIFICATION NUMBER |
|---|---|---|

| 8c. ADDRESS (City, State and ZIP Code)<br>1860 Wiehle Ave.<br>Reston, VA. 22090 | 10. SOURCE OF FUNDING NOS. | | | |
|---|---|---|---|---|
| | PROGRAM ELEMENT NO. | PROJECT NO. | TASK NO. | WORK UNIT NO. |

11. TITLE (Include Security Classification)
See Box 19.

12. PERSONAL AUTHOR(S)
Steven L. Skipper, B.S., Captain, USAF

| 13a. TYPE OF REPORT<br>MS Thesis | 13b. TIME COVERED<br>FROM _____ TO _____ | 14. DATE OF REPORT (Yr., Mo., Day)<br>1984 December | 15. PAGE COUNT<br>114 |
|---|---|---|---|

16. SUPPLEMENTARY NOTATION

| 17. | COSATI CODES | | 18. SUBJECT TERMS (Continue on reverse if necessary and identify by block number) |
|---|---|---|---|
| FIELD | GROUP | SUB. GR. | Communications Satellites |
| 22 | 02 | | Diversity Reception |
| 20 | 14 | | |

19. ABSTRACT (Continue on reverse if necessary and identify by block number)

Title:  ANALYSIS OF SPACE DIVERSITY TECHNIQUES
         FOR EHF SATELLITE DOWNLINKS

Thesis Chairman:  Kenneth G. Castor, Major, USAF

Approved for public release: IAW AFR 190-17.

Dean for Research and Professional Development.
Air Force Institute of Technology (AIC)
Wright-Patterson AFB OH 45433

| 20. DISTRIBUTION/AVAILABILITY OF ABSTRACT<br>UNCLASSIFIED/UNLIMITED ☒ SAME AS RPT. ☐ DTIC USERS ☐ | 21. ABSTRACT SECURITY CLASSIFICATION<br>UNCLASSIFIED | |
|---|---|---|
| 22a. NAME OF RESPONSIBLE INDIVIDUAL<br>Kenneth G. Castor, Major, USAF | 22b. TELEPHONE NUMBER<br>(Include Area Code)<br>513-255-3576 | 22c. OFFICE SYMBOL<br>AFIT/ENG |

DD FORM 1473, 83 APR          EDITION OF 1 JAN 73 IS OBSOLETE.          UNCLASSIFIED

This study investigated some of the diversity combining
techniques that can be used with a space diversity downlink
reception configuration to overcome the attenuation effects
of rainfall.  The diversity combining techniques selected
for development and analysis were selection, equal gain, and
maximal ratio combining.  Each of these techniques were con-
sidered with two different digital signaling schemes, 8-ary
phase-shift keying (PSK) and differentially encoded quadra-
ture PSK (DQPSK), to form six distinct diversity technique/
signaling scheme combinations.

The analysis was accomplished by deriving the probability
of bit error functions for 8-ary PSK and DQPSK and by devel-
oping the probability of density functions for each diversity
technique under the assumption of a slowly fading Rayleigh
channel.  By taking the integral from zero to infinity of the
product of the two functions for each diversity technique/
signaling scheme combination, the probability of bit error
was calculated for each specified combination. The number of
channels in the diversity system was varied to illustrate the
trade-off between the improvement of bit error performance
and cost.  The results show the theoretical benefits attrib-
uted to the diversity combining techniques that can be
employed in satellite communications systems. Additionally,
information is provided to estimate the rain attenuation
given the rain rate so that its effects on bit error per-
formance can be obtained and compared to the case of no rain
attenuation.

ORIGINATOR - SUPPLIED KEY WORDS INCLUDE:

# END

# FILMED

4-85

# DTIC